CONSTRUCTION MATERIALS CONSULTANTS, INC.

Petrographic Examinations and Air-Void Analyses of Four (4) Concrete Cores From PROJECT NAME

PROJECT NAME
ADDRESS
ADDRESS

Prepared for:
CLIENT

DATE
CMC NUMBER

Construction Materials Consultants, Inc.

Berkshire Center, Suite 104
4727 Route 30
Greensburg, PA 15601 USA
Phone: 724-834-3551
Fax: 724-834-3556
www.cmc-concrete.com

DATE

CLIENT CONTACT
CLIENT
ADDRESS
ADDRESS
ADDRESS

RE: PROJECT NAME; PROJECT NUMBER

Dear CLIENT CONTACT:

Construction Materials Consultants, Inc. (CMC) is pleased to provide the enclosed comprehensive report on 'Petrographic Examinations and Air-Void Analyses of Four (4) Concrete Cores From PROJECT BUILDING At PROJECT NAME'.

Results, opinions, and conclusions presented herein are based on the information and samples provided at the time of this investigation. We reserve the right to modify the report as additional information becomes available. Neither CMC nor its employees assume any obligation or liability for damages, including, but not limited to, consequential damages arising out of, or in conjunction with the use, or inability to use this resulting information.

Samples will be returned after submission of the report as requested. All reports are the confidential property of clients, and information contained herein may not be published or reproduced pending our written approval.

Please feel free to contact us with any additional questions. We look forward to providing our service again for your future projects.

Sincerely Yours,

CONSTRUCTION MATERIALS CONSULTANTS, INC.

Dipayan Jana, PG
President, Petrographer

DJ:jlh

TABLE OF CONTENTS

EXECUTIVE SUMMARY

Four concrete cores identified as Nos. C-1 through C-4 were received from the exterior façade & perimeter heating system of the PROJECT BUILDING in the PROJECT NAME. Core locations are south side ground level (for C-1), west side ground level (for C-2), north side 2nd level (for C-3), and east side 2nd level (for C-4). The purposes of this investigation are to determine the overall compositions, qualities, and conditions of concretes in the cores, and air contents and air void parameters of concretes. Petrographic examinations *a la* ASTM C 856 and air-void analyses *a la* ASTM C 457 were used to achieve these goals.

Based on detailed petrographic examinations, concretes in all four cores are found to be compositionally similar indicating use of same concrete mix across these core locations. Concretes are air-entrained, and made using: (i) crushed limestone coarse aggregates having nominal maximum sizes of $^3/_4$ in. (19 mm); (ii) natural siliceous-calcareous sand fine aggregates having nominal maximum sizes of $^3/_{16}$ in. (4.8 mm); (iii) Portland cements having estimated cement contents of 6 to $6^1/_2$ bags per cubic yard, and water-cement ratios of pastes of 0.50 to 0.55; and (vi) determined air contents of 5.4 to 7.1 percent.

Concretes in all cores are air-entrained having air-void systems consisting of numerous fine, discrete, spherical and near spherical entrained air voids, and a few coarse and irregularly shaped entrapped air voids. Concretes in cores C-1 from south side ground level and C-4 from east side 2nd level have overall higher air contents and finer air-void systems than the concretes from C-2 and C-3. Specific surfaces are all higher than the minimum recommended value of 600 in.^{2}/in.^{3}, and the air void-spacing factors are all less than the maximum recommended value of 0.0080 in.

Carbonation of concrete is measured to be higher than that normally found in a well-consolidated, well-cured concrete made using a reasonable water-cementitious materials ratio of 0.45 or less. Depths of carbonation measured on thin sections of cores are found to be: (i) as deep as 35 mm in C-1, (ii) merely 2 mm in the dense top grout in C-2, except along the visible vertical shrinkage-related crack on the grout where carbonation of paste along the crack walls has extended to a depth of 15 mm, (iii) 2 mm deep carbonation from the scarified concrete surface beneath the grout topping in C-2, (iv) 15 mm deep from the top surface of concrete in C-3, and (v) 22 mm deep in Core C-4. These depths are indicative of a concrete that has lesser resistance to penetration of atmospheric carbon dioxide and hence more permeability to CO_2 than desired for prevention of any carbonation-induced corrosion of reinforcing steel in concrete. Although there is no evidence of any corrosion of steel in Core C-4, which has a No. 4 reinforcing steel at a depth of 3 in. based on these deep carbonation depths, the possibility of such corrosion if steel reinforcement is present within the top 1 to 2 in. is present.

Along with the this evidence of deep carbonation, another microstructural evidence found in all four cores also indicate an inherent water-cement ratio of concrete that has not only increased permeability of concrete to CO_2 but also helped to form this microstructure. This evidence is the detection of fine, hair-like discontinuous microcracks that are detected in the paste fractions of all cores and are judged to be present at frequencies higher than that anticipated in a concrete made using a reasonable maximum water-cement ratio of 0.45. Deep carbonation and higher frequency of microcracking are thus both indicative of an inherent high water-cement ratio of concrete, which is consistent with the estimated values of 0.50 to 0.55. Composition, density, hardness, texture, lustre, and porosity of pastes, and appearance and behavior of cores during sectioning and lapping also corroborated the above conclusions.

A variation in overall air-void system of concrete between cores C-1/C-4 (better air-void systems) and C-2/C-3 (not as good as in the former two cores), along with a conclusion of an inherently higher water-cement ratio of concrete in all cores to cause deep carbonation and microcracking are the two issues discovered from this study. The effects of these issues on the short and long-term properties and performance of concrete, and durability however, are unknown.

INTRODUCTION

Reported herein are the results of detailed laboratory studies of four concrete cores received from CLIENT CONTACT of CLIENT. The concrete cores were, reportedly, taken from the Project: PROJECT NAME located at PROJECT LOCATION. Figure 2 shows the project location on a map found on the PROJECT website.

BACKGROUND INFORMATION

The following background information about the subject building was taken from the PROJECT website:

Figure 1: History of the PROJECT BULIDNG and a photograph of the building, taken from the PROJECT website.

Figure 2: Map of the PROJECT LOCATION from the PROJECT website (left) and a corresponding Google Map (right) showing the location of the building (circled) from which the samples were, reportedly, taken.

PURPOSES OF PRESENT INVESTIGATION

Based on the background information provided, the purposes of the present investigation are to determine:

a. The compositions, qualities, and overall conditions of concretes in the cores;
b. Evidence of any physical or chemical deterioration of concretes in the cores; and,
c. Determination of air contents and air-void parameters of concretes in the cores.

METHODOLOGIES

PETROGRAPHIC EXAMINATIONS

Petrographic examinations of four cores were done by following the methods of ASTM C 856 "Standard Practice for Petrographic Examination of Hardened Concrete." Details of petrographic examinations and sample preparation are described in Jana (1997a, b, 2001, 2004a, b, 2005a, b, 2006, 2007).

The steps of petrographic examinations include (Jana 2006):

i. Visual examinations of samples, as received;
ii. Low-power stereomicroscopical examinations of as-received, saw-cut and freshly fractured sections, and lapped cross sections of cores for evaluation of textures, and composition;
iii. Low-power stereomicroscopical examinations of air contents and air-void systems of concretes in the core;
iv. Examinations of oil immersion mounts in a petrographic microscope for mineralogical compositions of specific areas of interest;
v. Examinations of blue dye-mixed (to highlight open spaces, cracks, etc.) epoxy-impregnated large area (50 mm × 75 mm) thin sections of concretes in a petrographic microscope for detailed compositional and microstructural analyses;
vi. Photographing samples, as received and at various stages of preparation with a digital camera and a flatbed scanner; and,
vii. Photomicrographs of lapped sections and thin sections of samples taken from stereomicroscope and petrographic microscope, respectively to provide detailed compositional and mineralogical information of concretes.

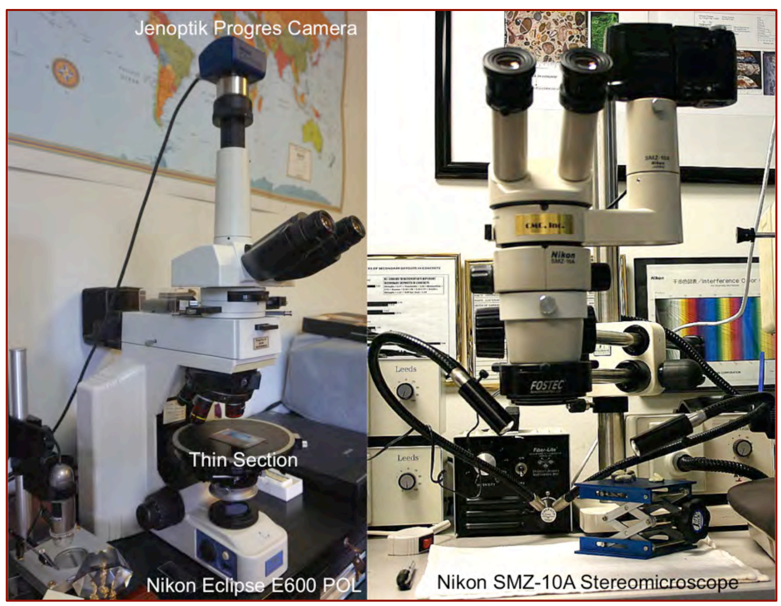

Figure 3: Nikon Eclipse E600POL Petrographic Microscope with Jenoptik Gryphax Camera and Nikon SMZ-10A Stereo-microscope used for petrographic examinations.

viii. A Nikon Eclipse 600 POL petrographic microscope attached to a Jenoptik Progres GRYPHAX high-resolution digital camera were used for petrographic examinations and collecting photomicrographs of thin sections of concretes (Figure 3). A Nikon SMZ-10A stereomicroscope (Figure 3) and an Olympus SZH stereomicroscope were used for examinations of fresh fractured and lapped sections and transmitted-light examinations of thin section, respectively.

AIR-VOID ANALYSES

The cores were tested and examined by using the ASTM Standard Practice of air-void analysis by following the modified point count method, as mentioned in ASTM C 457 "Standard Test Method for Microscopical Determination of Parameters of the Air-Void System in Hardened Concrete," where the steps followed during air-void analyses are given below. Details of sample preparation for air-void analysis are given in Jana 2007.

a. The Velmex point-count device used in the analysis (see Figure 4) comprised a platform connected to E-W and N-S lead screws and designed in such a way that a lapped concrete sample placed on the stage can be moved smoothly and uniformly through equal distances by turning of the screws. It was ensured that the total possible translation of the stage was at least 100 mm (4.0 in.) in each direction. Lead screws were fitted with notched wheels and stopping devices, such that with each rotation of the screws the operator can detect a click when a stop position was reached. It was ensured that the intervals between the stops correspond to a translation of the stage a distance of 0.025 to 0.64 to 5.0 mm (0.025 to 0.200 in.). The magnitude of the average translation of the stage between stops was determined to the nearest 0.03 mm (0.001 in.). A total of six digital counters were used for calculating aggregates, paste, entrained and entrapped voids, and total voids intercepted during the traverse.

b. A high-resolution Olympus SZH stereomicroscope attached to a high-resolution digital microscope camera was used to capture live image of the lapped concrete surface on the PC screen.

c. A lapped section of concrete was place on the stage of the point-count device. Using the spirit level, the prepared surface was leveled with the leveling device so that the surface may be traversed and microscopically examined with a minimum of refocusing. Lamp was adjusted so the beam evenly illuminated the field of view of the microscope and was incident upon the surface at a low angle, so the air voids were demarked by a shadow. Superimposed in the computer screen was the index point of the cross hairs to pinpoint the area to be counted. A magnification not less than 50X was used and wasn't changed during the course of the analysis. For a rectangular lapped section, the index was placed near an upper corner (for a circular section, it is usually placed near the top) and at one end of the initial traverse. The stopping device was positioned at a stop or click position at the beginning of the traverse. The initial stops for each traverse line were not included in the total number of stops or in the number of stops for any component. Zeroed all counters. By operation of the E-W lead screw, caused movement of the stage and specimen while simultaneously scrutinizing the surface. At each click stop, except not at the beginning of any traverse line, paused and examined the field of view, and recorded on the appropriate counter the material or phase on which the index point was superimposed. Normally used one counter for air voids, one for paste, and one for all other phases (or a totaling counter). Other components (fine and coarse aggregate, for example—if they are lithologically distinguishable) of the concrete were determined with the use of additional counters. Continued in this way along the line until a last stop is reached just within the prepared area, but close to its edge. When the end of the line is reached, turned off the totaling counter. Reversed the E-W lead screw and proceeded back along the same line, recording on another counter each air void intersected, whether or not a stop has occurred within the air void. Terminated the void counting just before the initial stop. Took extreme care to determine whether a section of an air void was intersected by the movement of the index when the line of traverse is nearly tangent to the void section. The results can be affected significantly by consistent error in this respect. If the periphery of an air void was crumbled or rounded, estimated the position of the true periphery in the plane of the surface by extrapolation of the surface contour of the air void. If the examination was being made to determine only the air content of the concrete, the number of air voids intersected by the line of traverse need not be determined. By means of the N-S lead screw, shifted the concrete specimen at right angles to the direction of traverse an appropriate distance. Spaced the segments of the traverse so as to cover the whole prepared surface and achieved at least the minimum length of traverse and the minimum number of points specified in C 457. Proceeded along the new line of traverse as before, and so on, for all segments of the total traverse and for all sections prepared from a sample of concrete so as to comply with the requirements of this test method.

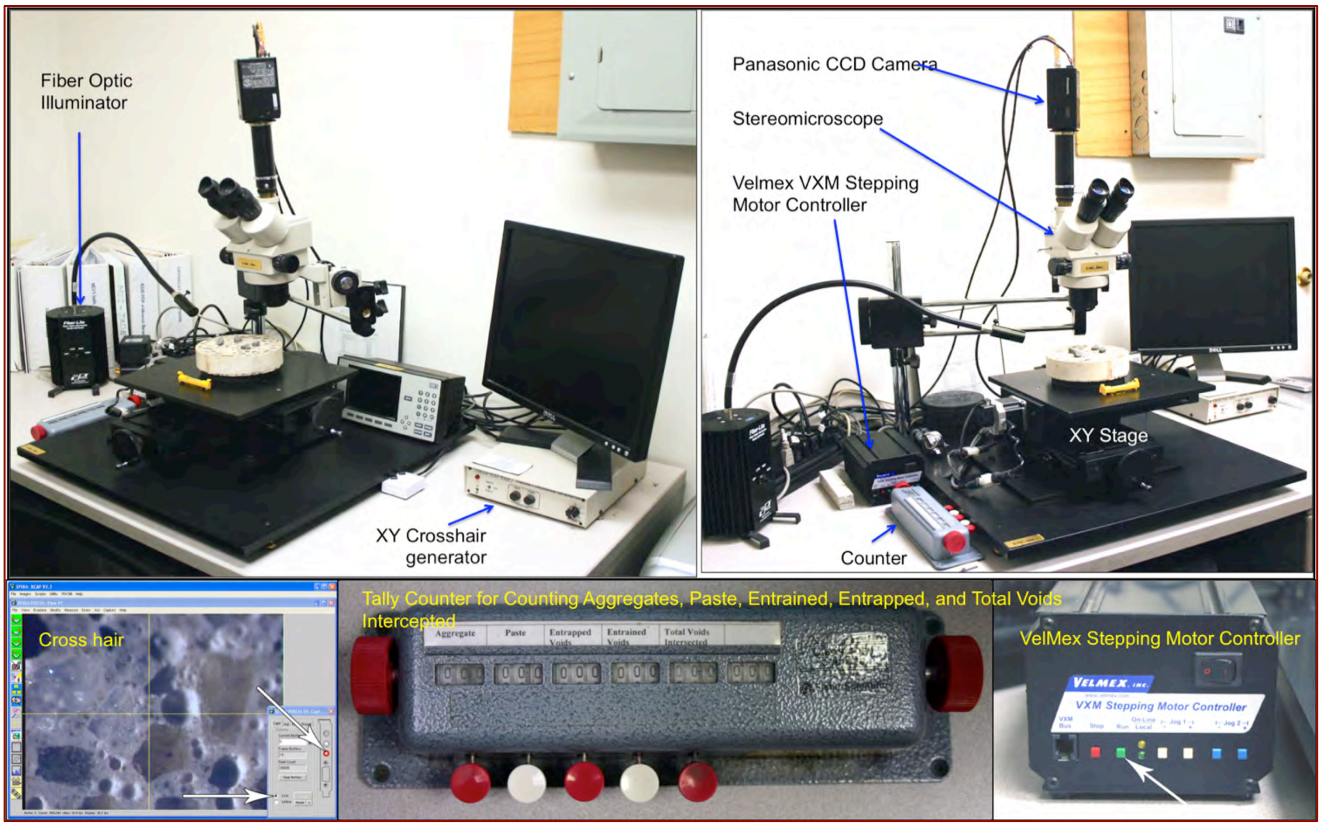

Figure 4: Set-up in the CMC laboratory for air-void analysis in hardened concrete by the modified point count method of ASTM C 457.

d. Minimum length of traverse and minimum number of points for the modified point count method were: (a) 2540 mm (100 in.) and 1500 points for $1\frac{1}{2}$-in. nominal size aggregate, (b) 2413 mm (95 in.) and 1425 points for 1-in. nominal size aggregate, (c) 2286 mm (90 in.) and 1350 points for $\frac{3}{4}$-in. nominal size aggregate, (d) 2032 mm (80 in.) and 1200 points for $\frac{1}{2}$-in. nominal size aggregate, and (e) 1905 mm (75 in.) and 1125 points for $\frac{3}{8}$-in. nominal size aggregate.

e. Air-void parameters were calculated by using the equations provided in C 457.

SAMPLES

PHOTOGRAPHS, IDENTIFICATION, INTEGRITY, AND DIMENSIONS

Figure 5 shows the four cores, as received. The identifications of each core, nominal diameters, nominal lengths, and overall conditions as received are shown in the following Table 1.

Sample ID	Diameter	Length	Top surface conditions	Bottom surface conditions	Cracks/Joints/ Large Voids	Reinforcing Steel	Integrity
C-1 RT1461 South Side, Ground Level	$3^3/_4$ in. (92 mm)	$8^3/_4$ in. (220 mm)	Smooth, flat, floated, chipped edges due to drilling	Fresh Fractured	Saw-cut sections removed from cylindrical side from $^1/_4$ in. (7 mm) to $2^1/_4$ in. (58 mm) depths	None	Intact
C-2 RT1461 West Side, Ground Level	$3^3/_4$ in. (92 mm)	8 in. (203 mm)	Smooth, flat, finished, microcracking	Formed with impressions of formwork element	Saw-cut sections removed from cylindrical side from $^1/_4$ in. (7 mm) to $2^1/_4$ in. (58 mm) depths	None	Intact
C-3 RT1461 North Side, 2nd Level	$3^3/_4$ in. (92 mm)	$8^1/_4$ in. (210 mm)	flat, formed, rough, weathered	Fresh Fractured	Saw-cut sections removed from cylindrical side from $^1/_4$ in. (7 mm) to $2^1/_4$ in. (58 mm) depths	None	Intact
C-4 RT1461 East Side, 2nd Level	$3^3/_4$ in. (92 mm)	$9^1/_2$ in. (240 mm)	Flat, formed, rough, weathered	Fresh fractured and formed concave surface with ridged impressions at $^1/_8$ in. (4 mm) intervals with trace remains of paper	Saw-cut sections removed from cylindrical side from $^1/_4$ in. (7 mm) to $2^1/_4$ in. (58 mm) depths	No. 4 reinforcing steel at a depth of 3 in. (90 mm), and an impression of a reinforcing steel at a depth of $1^3/_4$ in. (45 mm) from the top surface	Intact

Table 1: Dimensions, end surfaces, and conditions of the four concrete cores, as received.

END SURFACES

The top exposed surfaces of are smooth, flat, finished. The bottom surfaces are formed in C-2 and C-4, and, fresh fractured in C-1 and C-3. Table 1 above and Figure 5 provide detailed descriptions and photos of end surfaces of individual cores, as received.

CRACKING & OTHER VISIBLE DISTRESS, IF ANY

All four cores showed portions of concrete removed from depths of $^1/_4$ in. (7 mm) to $2^1/_2$ in. (58 mm) from the top surfaces, as described in Table 1 and seen in the middle column along the top side cylindrical surfaces of cores in Figure 5. There are no major cracks, joints, or voids present in the cores received. All four cores were received in intact conditions, except for the above-mentioned partially removed portions.

Figure 5: Overview of concrete cores received. For each core: left photo shows the top exposed surface, right photo shows bottom surfaces, and middle photos show side cylindrical views of the cores, as received. All four cores show some removal of sample from the top 2 inches probably due to some other (e.g., chloride content) testing not requested in this study.

EMBEDDED ITEMS

One of the four cores received, Core No. C-4, contains a No. 4 reinforcing steel at a depth of 3 in. (90 mm) from the top surface, and an impression of a reinforcing steel at a depth of $1^3/4$ in. (45 mm) from the top surface. There are no other reinforcing steels, fibers, wire mesh, or embedded items found in the cores examined.

RESONANCE

The cores have a ringing resonance, when hammered.

PETROGRAPHIC EXAMINATIONS

COARSE AGGREGATES

Coarse aggregates are crushed limestones, having nominal maximum sizes of $^3/4$ in. (19 mm). Particles are angular, moderately dense to dense, moderately hard to hard, light to dark gray, massive-textured, equidimensional to elongated, unaltered, uncoated, and uncracked. Rock types detected are microcrystalline limestone (micrite), fossiliferous limestone (biomicrite), dolomitic limestone, argillaceous varieties of limestone, limestone with quartz inclusions, dolomite etc. which are shown in photomicrographs of lapped and thin sections.

Coarse aggregate particles are well-graded and well-distributed (Figures 6 through 9). Relative volumes of crushed stone coarse aggregates, however, showed some variations as seen in lapped cross sections in Figures 6 through 9 i.e. Core C-3 has the highest volume, C-2 has the lowest volume, and C-1 and 4 have somewhat intermediate volumes of coarse aggregates. There is no evidence of alkali-aggregate reaction of coarse aggregate particles in the samples. Coarse aggregate particles have been physically and chemically sound during their service in the concretes.

FINE AGGREGATES

Fine aggregates are natural siliceous-calcareous sands having nominal maximum sizes of $^3/8$ in. (9.5 mm). Particles contain major amounts of quartz and quartzite, and moderate amounts of feldspar, chert, granite, quartz siltstone, ferruginous siltstone, sandstone, greywacke, shale, mafic minerals, and ferruginous rocks. Particles are variably colored, subrounded to subangular, variably dense and colored, hard, equidimensional to elongated, unaltered, uncoated, and uncracked.

Fine aggregate particles are well-graded and well-distributed. There is no evidence of alkali-aggregate reaction of fine aggregate particles. Fine aggregate particles have been sound during their service.

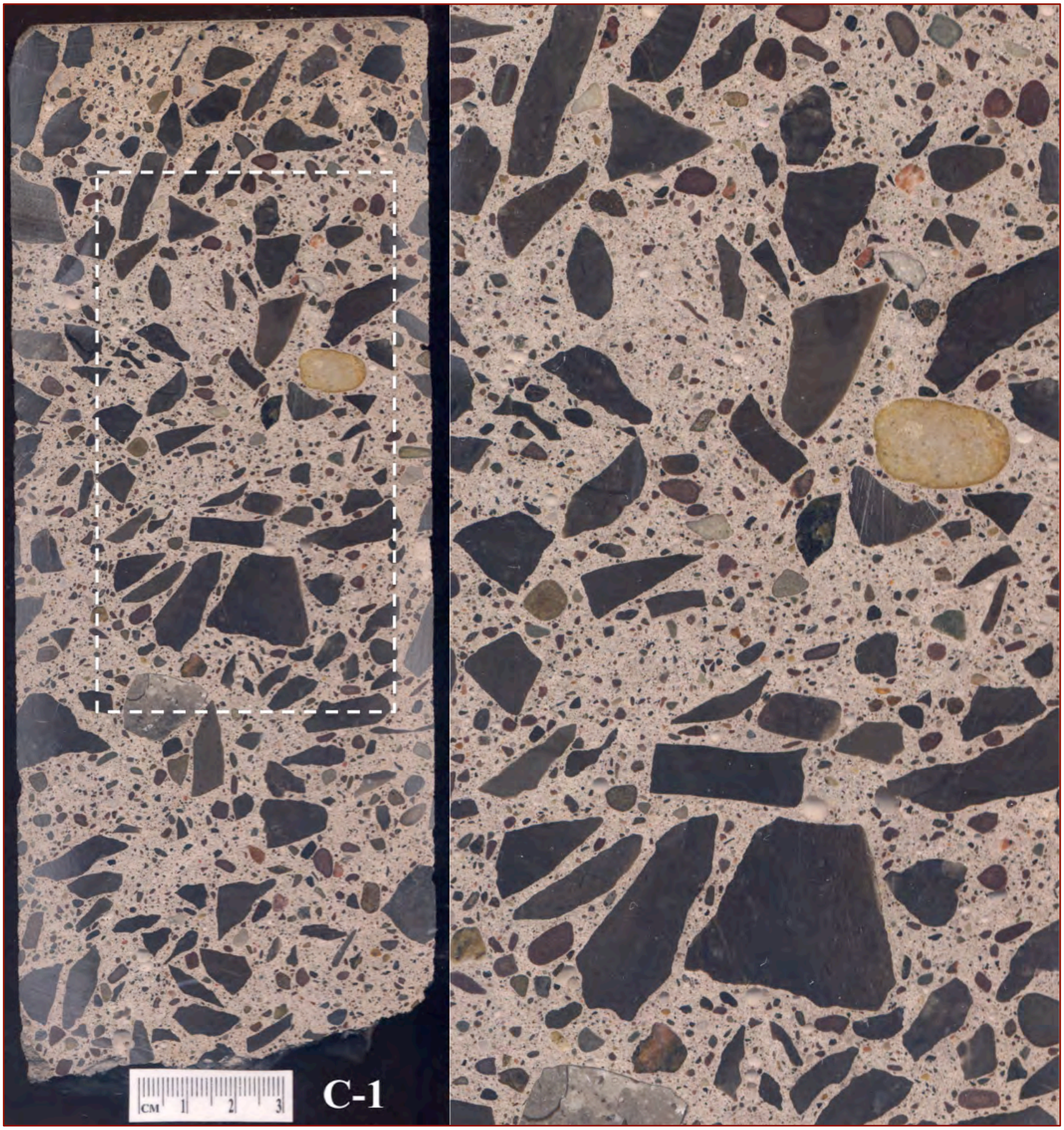

Figure 6: Lapped cross section of the core C-1 showing the good grading and well-distribution of crushed stone coarse and natural sand fine aggregates and dense, well-consolidated nature of concrete. The boxed area in the left photo is enlarged at right.

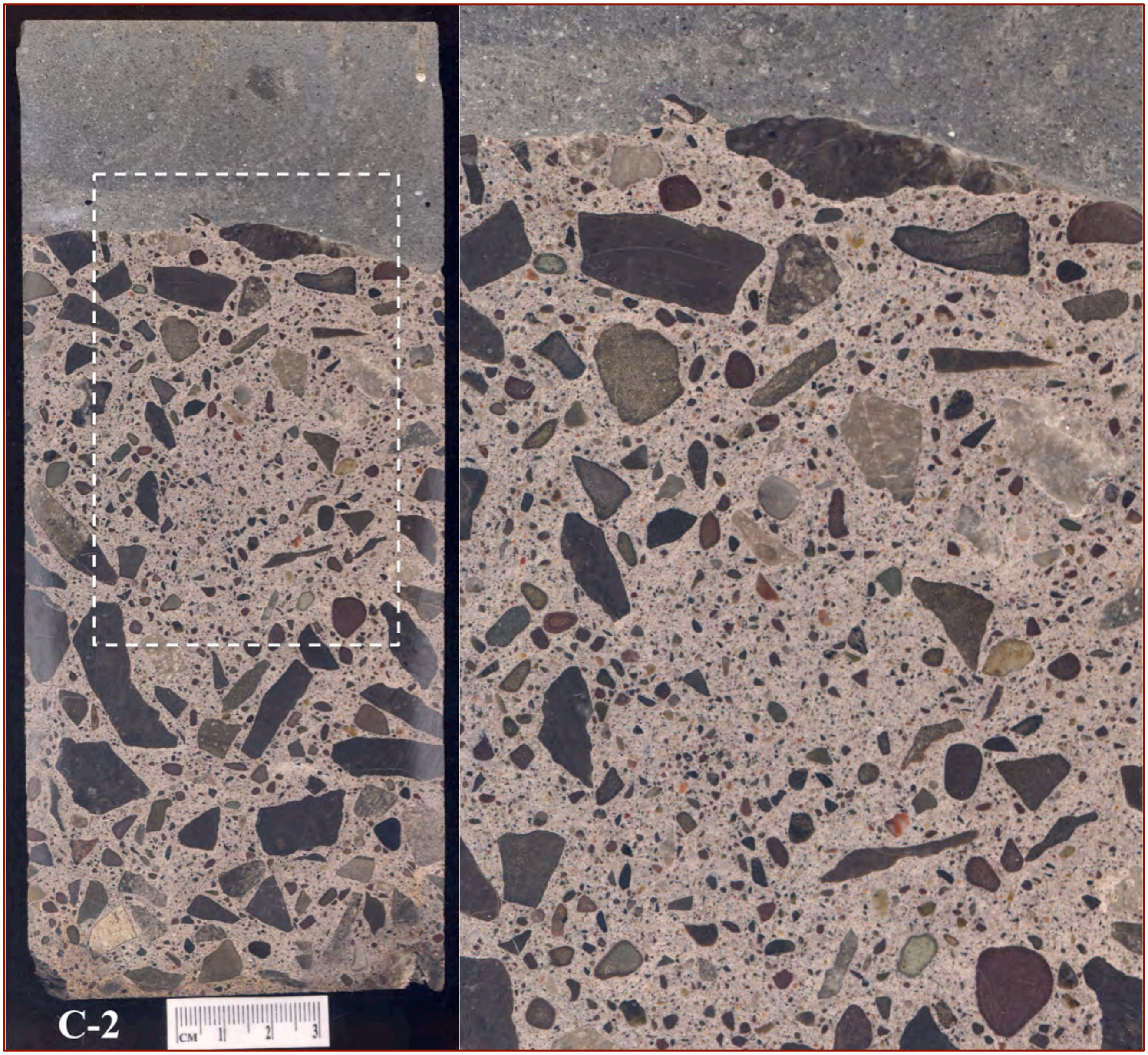

Figure 7: Lapped cross section of the core C-2 showing the good grading and well-distribution of crushed stone coarse and natural sand fine aggregates and dense, well-consolidated nature of concrete. The boxed area in the left photo is enlarged at right. Notice the intimate bond between the dense, dark gray grout at the top and concrete substrate.

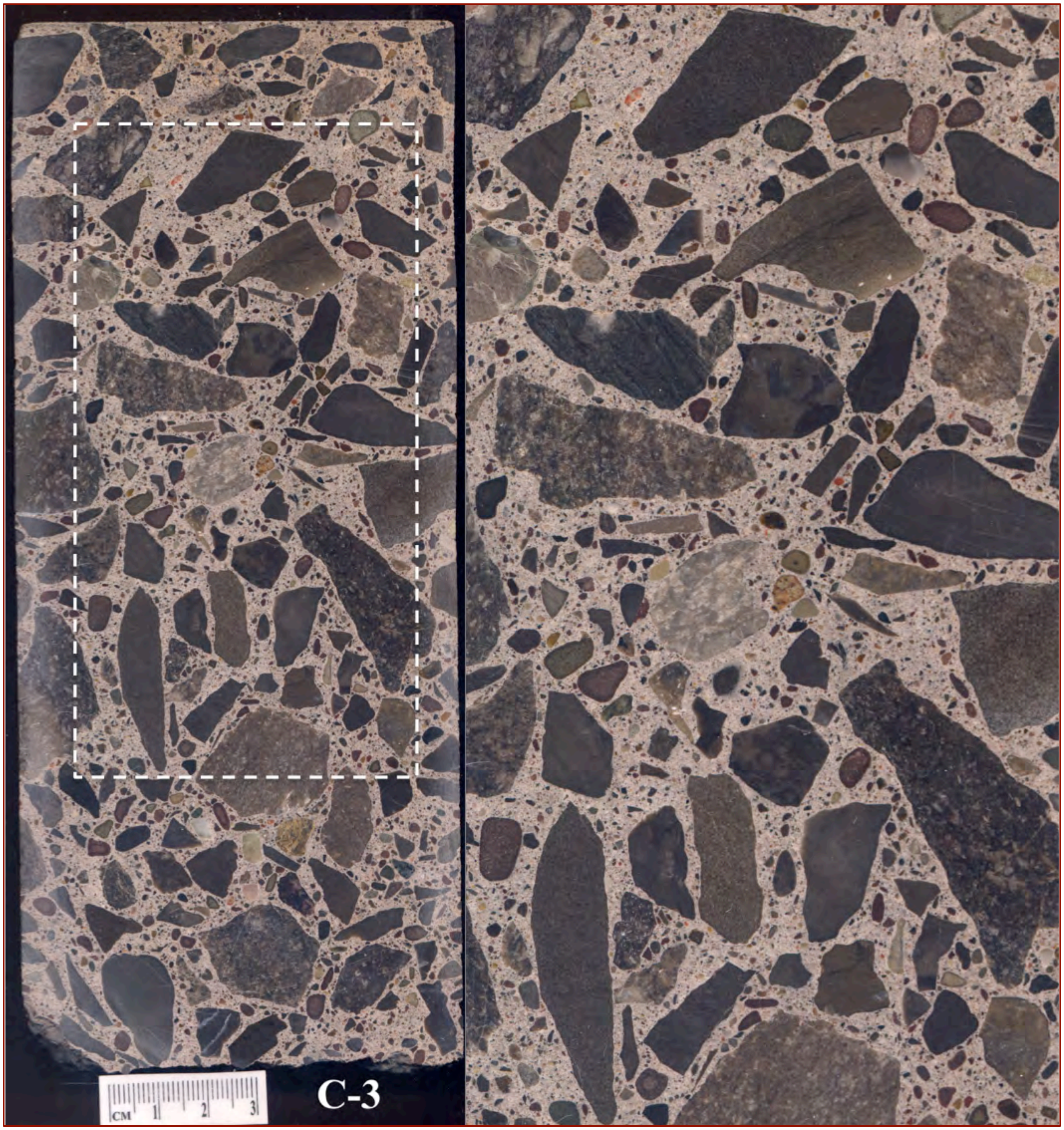

Figure 8: Lapped cross section of the core C-3 showing the good grading and well-distribution of crushed stone coarse and natural sand fine aggregates and dense, well-consolidated nature of concrete. The boxed area in the left photo is enlarged at right.

Figure 9: Lapped cross section of the core C-6 showing the good grading and well-distribution of crushed stone coarse and natural sand fine aggregates and dense, well-consolidated nature of concrete. The boxed area in the left photo is enlarged at right.

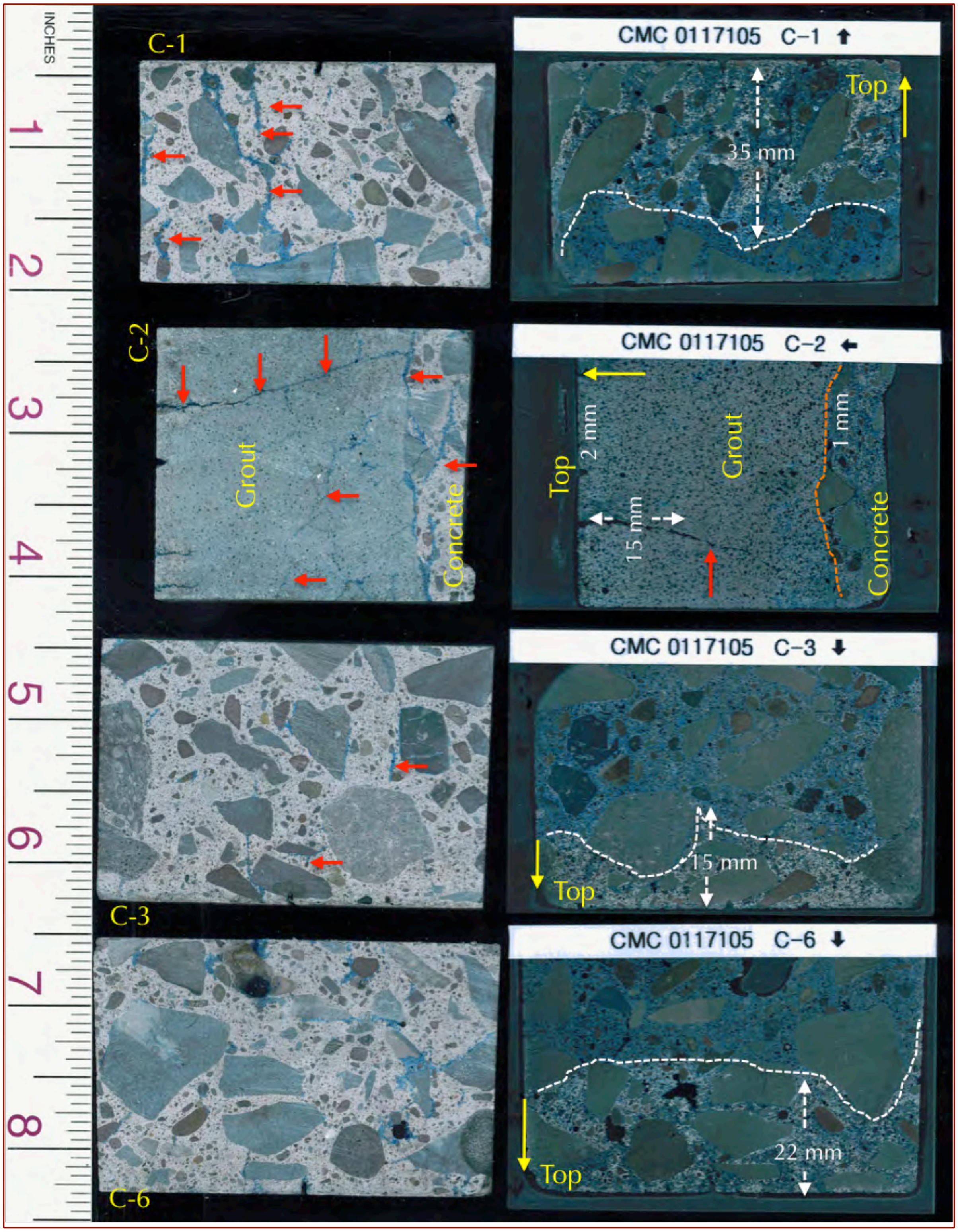

Figure 10: Blue dye-mixed epoxy-impregnated thin sections of four cores (shown along with the corresponding residues left after thin section preparations on the left side of thin sections). Thin sections were 50 by 75 mm in size and were used for examinations in Nikon petrographic microscope. White dashed lines show the depths of carbonation of pastes along with the measured depths shown. Red arrows show some discontinuous microcracks. The top directions of cores are marked with yellow arrows.

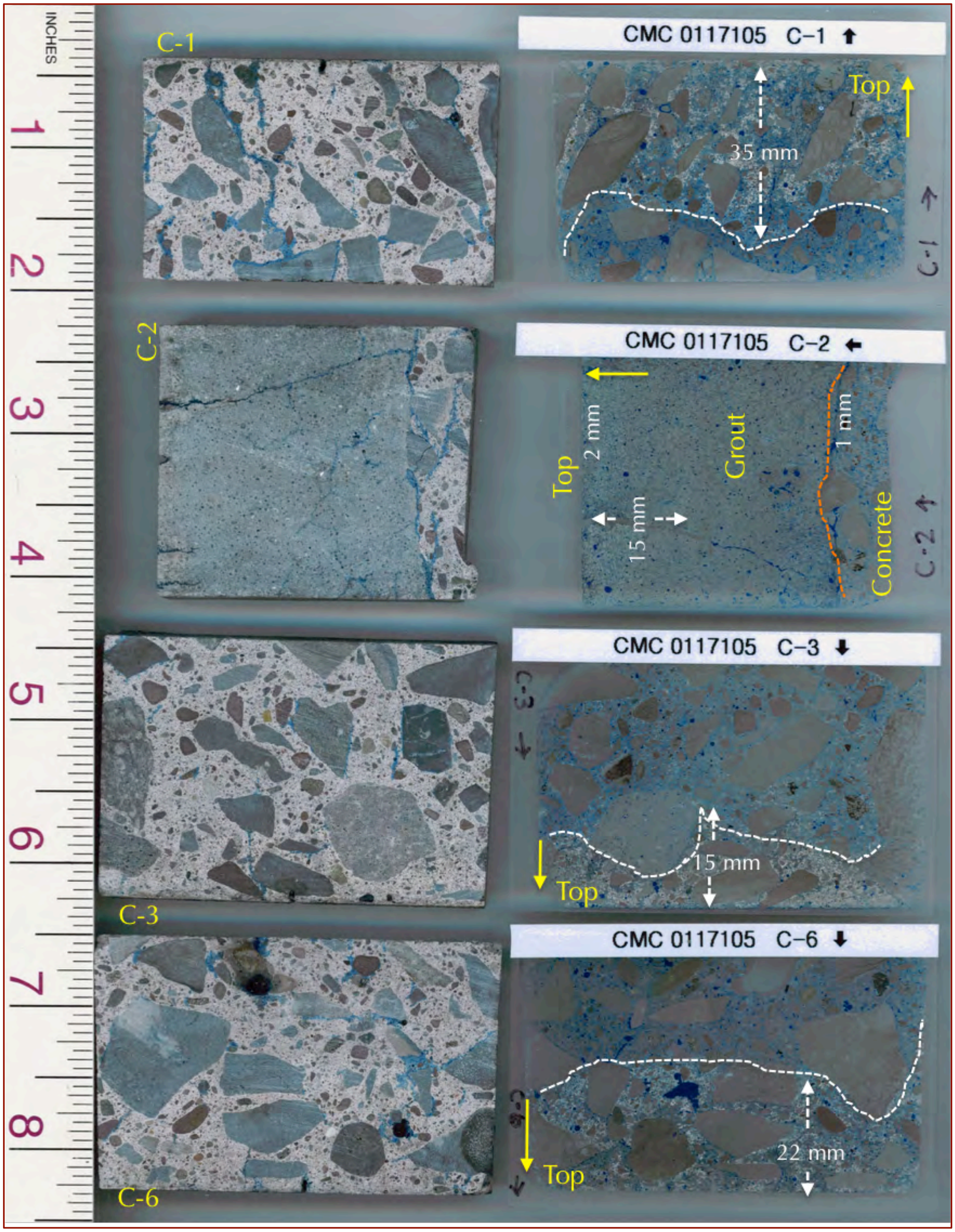

Figure 11: Same as Figure 10 but thin sections are shown against white background. White dashed lines show the depths of carbonation of pastes along with the measured depths shown. The top directions of cores are marked with yellow arrows. Concrete showed 35 mm deep carbonation in C-1, 2 mm deep in the grout except along the vertical macro crack where carbonation extended to 15 mm, 15 mm deep carbonation in C-3, and 22 mm deep carbonation in C-6.

The following Table summarizes properties of coarse and fine aggregates determined from the samples:

Properties and Compositions of Aggregates	C-1 South Side, Ground Level	C-2 (Concrete) West Side, Ground Level	C-3 North Side, 2nd Level	C-4 East Side, 2nd Level
Coarse Aggregates				
Types	Crushed limestone	Crushed limestone	Crushed limestone	Crushed limestone
Nominal maximum size (in., mm)	$^{3}/_{4}$ in. (19 mm)	$^{3}/_{4}$ in. (19 mm)	$^{3}/_{4}$ in. (19 mm)	$^{3}/_{4}$ in. (19 mm)
Rock Types	Microcrystalline limestone (micrite), fossiliferous limestone (biomicrite), dolomitic limestone, argillaceous varieties of limestone, limestone with quartz inclusions, dolomite			
Angularity, Density, Hardness, Color, Texture, Sphericity	Angular, moderately dense to dense, moderately hard to hard, light to dark gray, massive-textured, equidimensional to elongated			
Cracking, Alteration, Coating	Unaltered, Uncoated, and Uncracked			
Grading & Distribution	Well-graded and Well-distributed			
Soundness	Sound	Sound	Sound	Sound
Alkali-Aggregate Reactivity	None	None	None	None
Fine Aggregates				
Types	Natural siliceous-calcareous sand – compositionally similar in all three cores			
Nominal maximum size (in., mm)	$^{3}/_{8}$ in. (9.5 mm)	$^{3}/_{8}$ in. (9.5 mm)	$^{3}/_{8}$ in. (9.5 mm)	$^{3}/_{8}$ in. (9.5 mm)
Rock Types	Major amounts of quartz and quartzite, and moderate amounts of feldspar, chert, granite, quartz siltstone, ferruginous siltstone, sandstone, greywacke, shale, mafic minerals, and ferruginous rocks			
Cracking, Alteration, Coating	Variably colored, subrounded to subangular, dense, hard, equidimensional to elongated			
Grading & Distribution	Well-graded and Well-distributed			
Soundness	Sound	Sound	Sound	Sound
Alkali-Aggregate Reactivity	None	None	None	None

Table 2: Properties of coarse and fine aggregates of concretes in the cores.

PASTES

Properties and compositions of hardened cement pastes are summarized in Table 3 and shown in Figures 12 through 23. Pastes are medium beige, moderately dense and moderately hard, freshly fractured surfaces have subvitreous lusters and subconchoidal textures. Residual and relict Portland cement particles are present and estimated to constitute 8 to 10 percent of the paste volumes. Hydration of Portland cement is normal. There is no evidence of the presence of fly ash, slag or other pozzolanic or cementitious admixtures in the cores.

Properties and Compositions of Paste	C-1 South Side, Ground Level	C-2 (Concrete) West Side, Ground Level	C-3 North Side, 2nd Level	C-4 East Side, 2nd Level
Color, Hardness, Porosity, Luster	Medium beige, moderately dense and moderately hard; Subvitreous – compositionally similar in all cores			
Residual Portland Cement Particles	Normal, 8 to 10 percent by paste volume			
Calcium hydroxide from cement hydration	Normal, 10 to 14 percent by paste volume			
Pozzolans, Slag, etc.	None	None	None	None
Water-cementitious materials ratio (*w/cm*), estimated	0.50 to 0.55, uniform throughout the depth	0.50 to 0.55, uniform throughout the depth	0.50 to 0.55, uniform throughout the depth	0.50 to 0.55, uniform throughout the depth
Portland cement contents, estimated (bags of portland cement per cubic yard)	6 to $6^1/_2$	6 to $6^1/_2$	6 to $6^1/_2$	6 to $6^1/_2$
Secondary Deposits	None	None	None	None
Depth of Carbonation (maximum depth measured on thin sections), mm	35 mm from the top of concrete	2 mm from top of grout, except along the major visible surface crack where carbonation extended to 15 mm, 1 to 2 mm from the concrete top from grout-concrete interface	15 mm from the top of concrete	22 mm from the top of concrete
Microcracking	Sporadic shrinkage-related microcracks are detected in the paste fractions of concretes in all cores (Figures 12 through 23); grout in Core C-2 has microcracks in paste			
Aggregate-paste Bond	Tight	Tight	Tight	Tight
Bleeding, Tempering	None	None	None	None
Chemical deterioration	None	None	None	None

Table 3: Proportions and composition of hardened cement pastes.

Overall similar compositions of pastes along with compositional similarities of coarse and fine aggregates in all cores indicate use of same concrete mix at the locations of all four cores that had incorporated crushed limestone coarse aggregate, natural siliceous-calcareous sand fine aggregate, Portland cement, and air entrainment.

The measured depths of carbonation of pastes in all cores are deeper than the normal for a well-consolidated concrete made with a reasonable water-cement ratio, which has been cured adequately. These deep carbonations are indicative of an inherent high water-cement ratio that has increased the permeability of concrete paste to atmospheric carbon dioxide. There is no evidence of poor consolidation of concrete in any core.

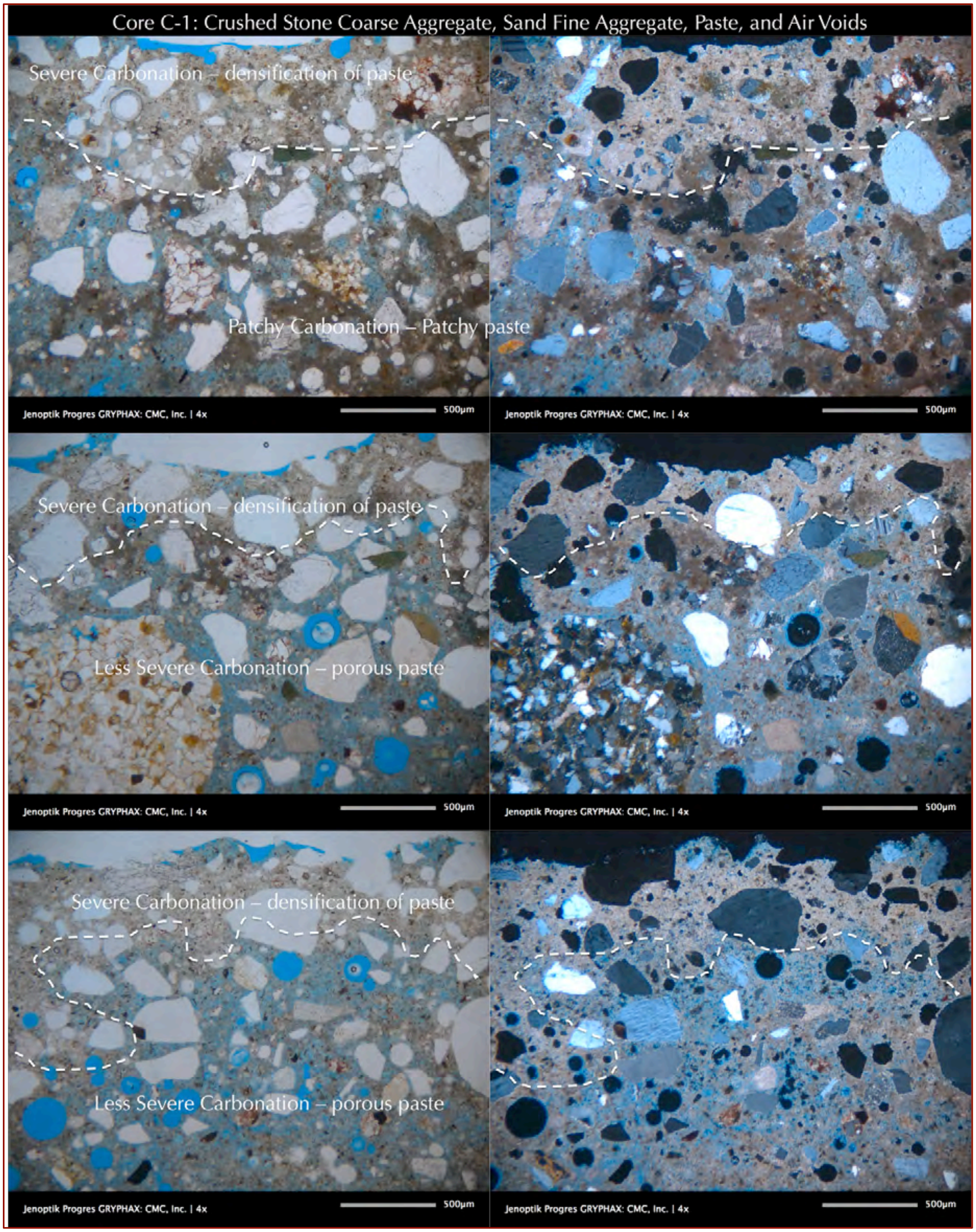

Figure 12: Photomicrographs of blue dye-mixed epoxy-impregnated thin section of Core C-1 from South Side, Ground Level showing: (a) severe carbonation and carbonation-induced densification of paste at the top 0.5 to 1.0 mm (all three rows), (b) relatively less carbonation and patchy-textured carbonated and non-carbonated patches of paste beneath the top 0.5 mm (top row and some in the middle row), (c) relatively porous but still carbonated paste beneath the patchy-textured paste at a depth beneath 1 mm (middle and bottom rows). Dashed lines separate the severely carbonated top 0.5 mm skin from the rest of the carbonated surface region. Left photos were taken at PPL and right ones at corresponding XPL modes in a petrographic microscope. Also notice crushed limestone coarse aggregate, natural siliceous-calcareous sand fine aggregate, Portland cement paste, and air voids that are highlighted by the blue dye-mixed epoxy.

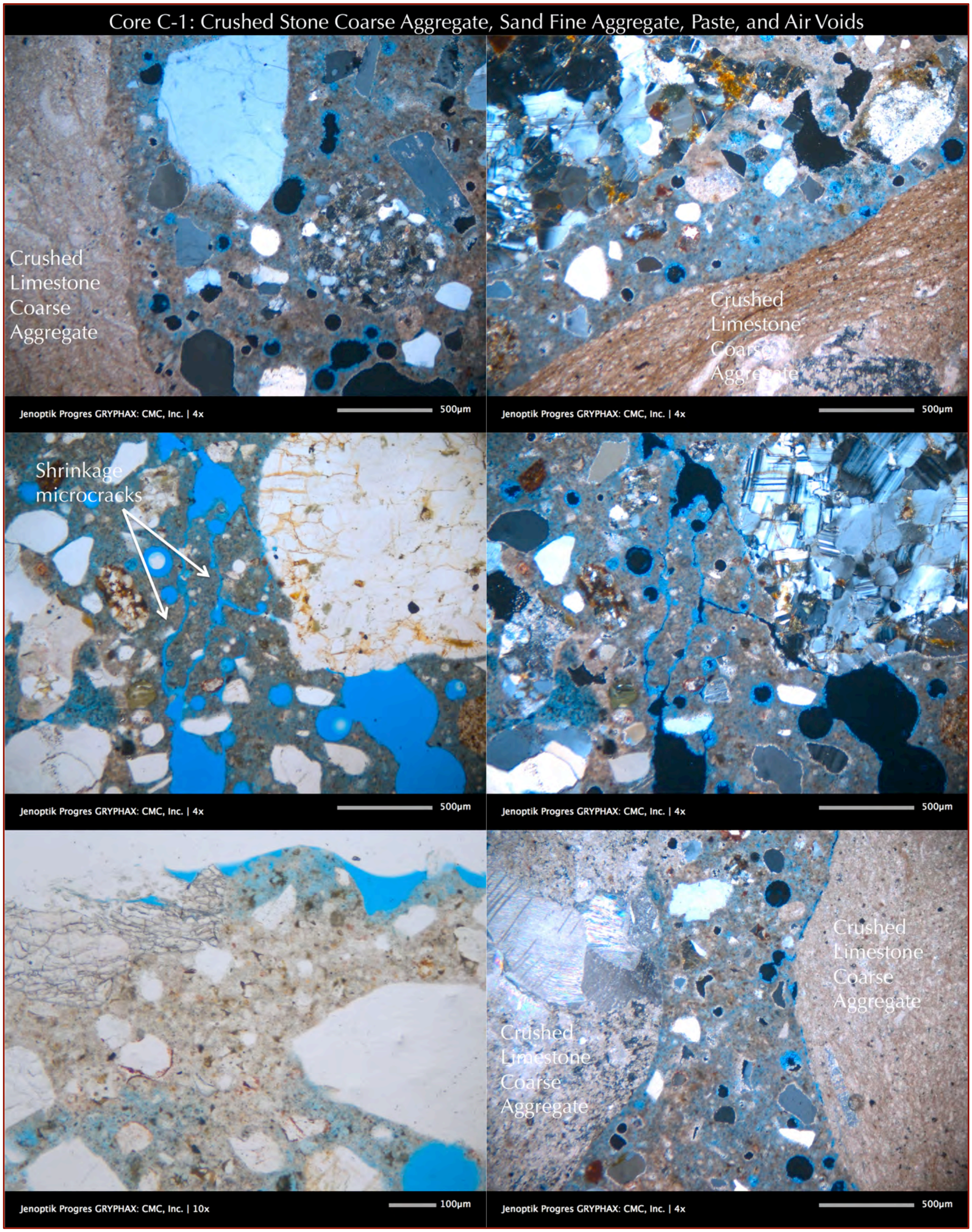

Figure 13: Photomicrographs of blue dye-mixed epoxy-impregnated thin section of Core C-1 from South Side, Ground Level showing: (a) carbonated surface region of paste (all three rows), and (b) fine, hair-like, discontinuous shrinkage microcracks in paste some are marked with arrows (middle row). Left photos in middle and bottom rows were taken at PPL and right ones at corresponding XPL modes in a petrographic microscope. Also notice crushed limestone coarse aggregate, natural siliceous-calcareous sand fine aggregate, Portland cement paste, and air voids that are highlighted by the blue dye-mixed epoxy.

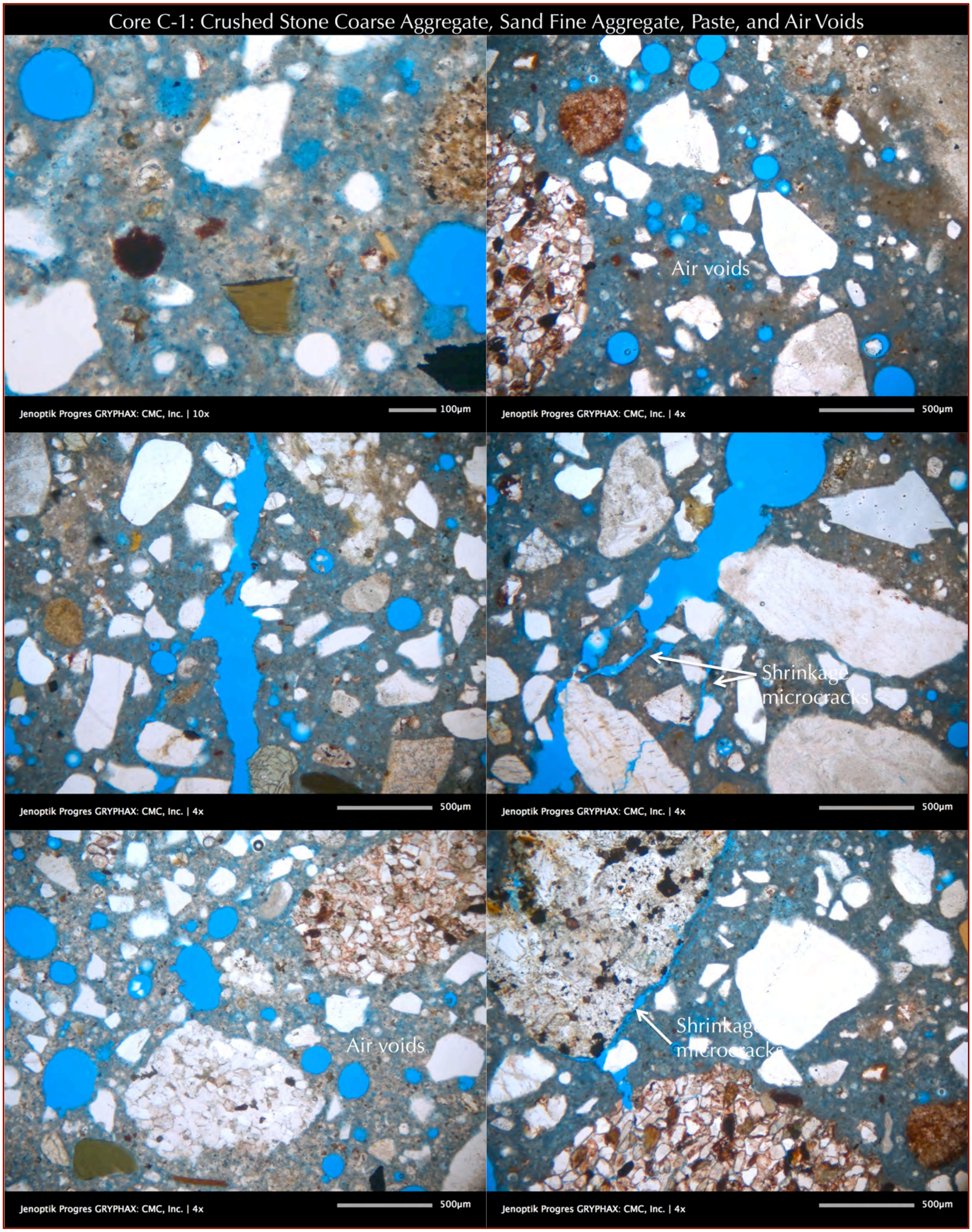

Figure 14: Photomicrographs of blue dye-mixed epoxy-impregnated thin section of Core C-1 from South Side, Ground Level showing: (a) fine, hair-like, discontinuous shrinkage microcracks in paste, some are marked with arrows (middle and bottom rows), and (c) distribution of entrained air voids that are highlighted by the blue dye-mixed epoxy.

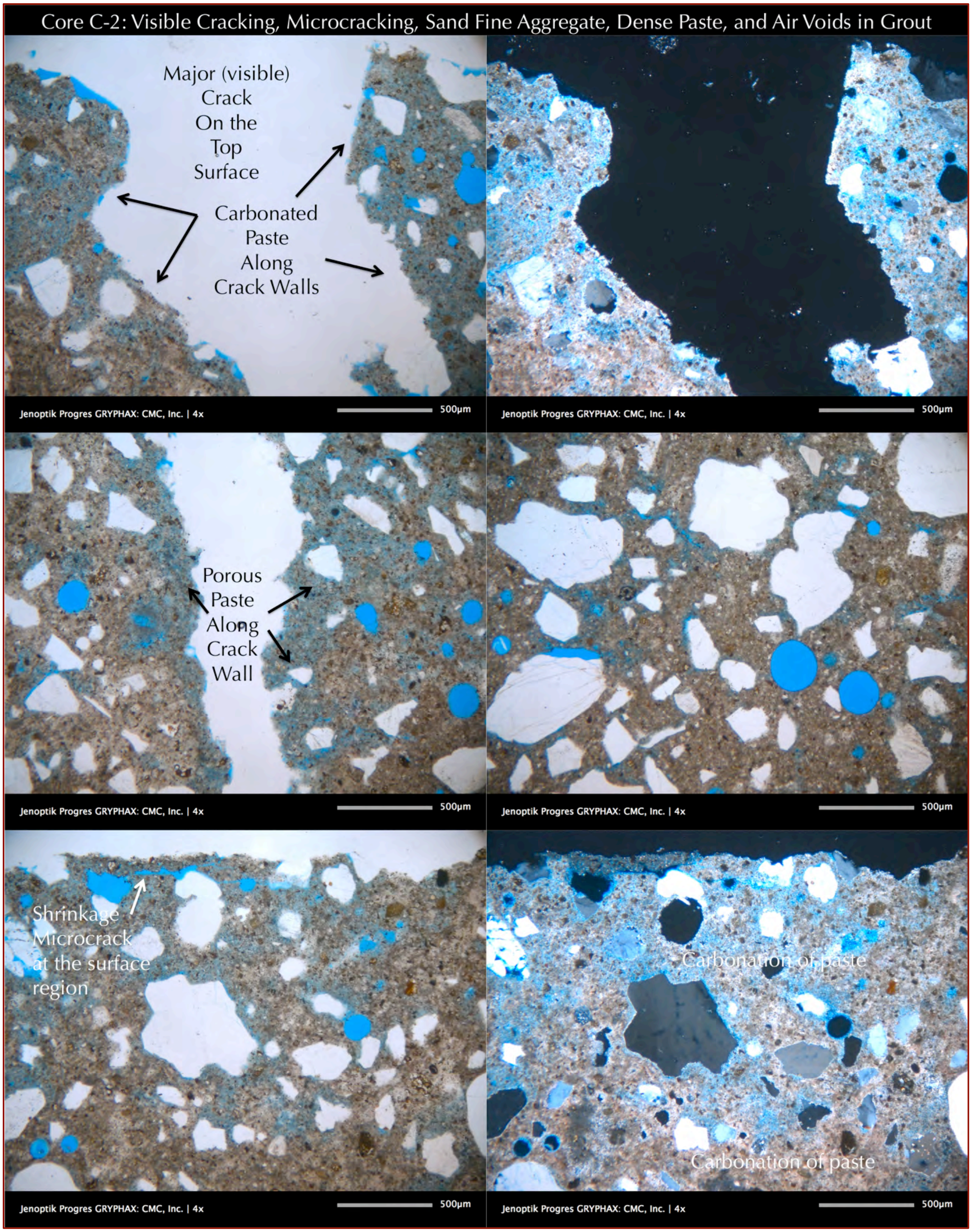

Figure 15: Photomicrographs of blue dye-mixed epoxy-impregnated thin section of Core C-2 from West Side, Ground Level showing: (a) carbonated surface region of paste in the grout along the major visible crack at the top surface (top row), (b) relatively porous paste along the major crack (middle row); (c) fine, hair-like, discontinuous shrinkage microcracks in paste in the grout at the carbonated surface region some are marked with arrows (bottom row). Left photos in top and bottom rows were taken at PPL and right ones at corresponding XPL modes in a petrographic microscope. Also notice crushed sand fine aggregate, dense Portland cement paste, and air voids that are highlighted by the blue dye-mixed epoxy.

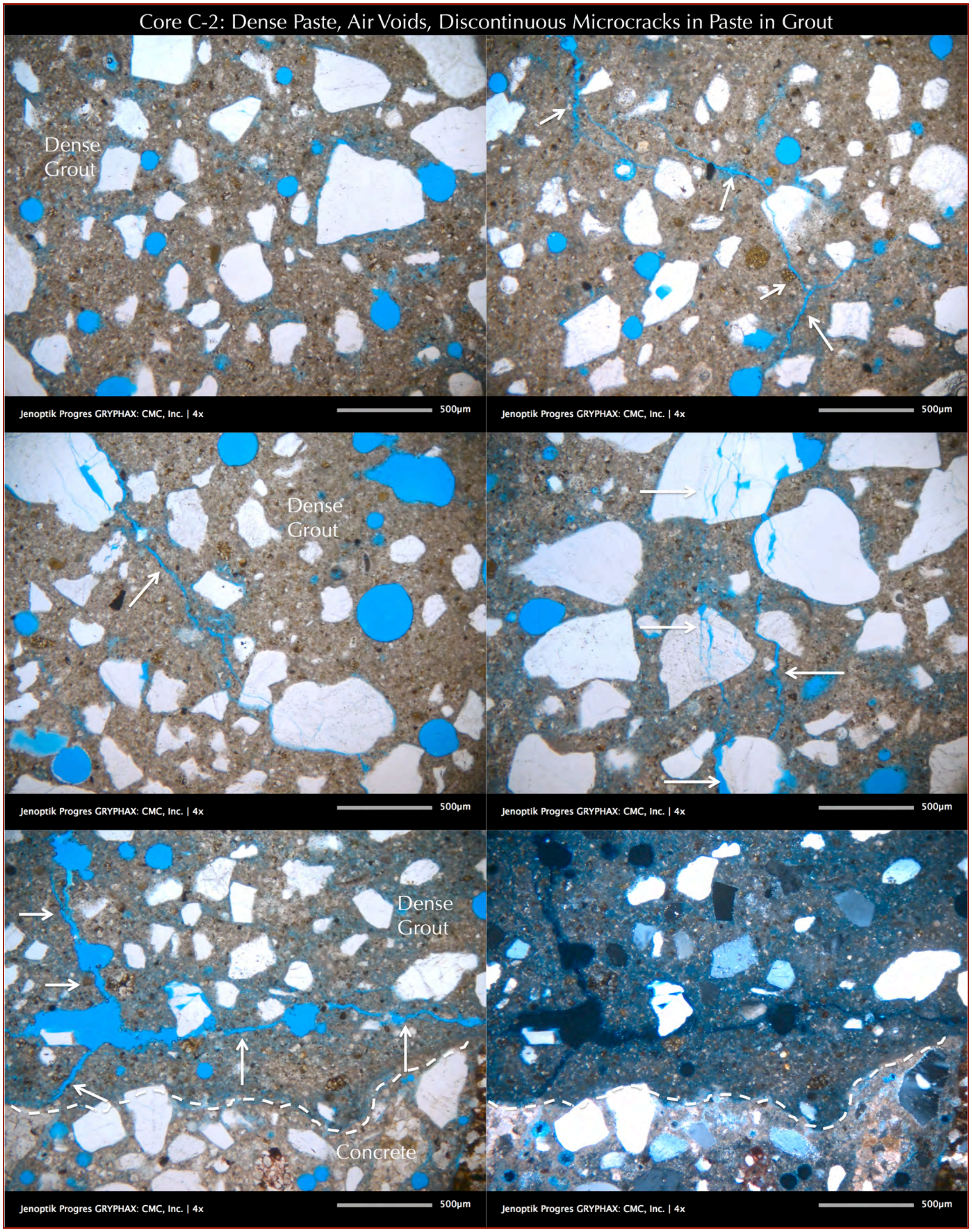

Figure 16: Photomicrographs of blue dye-mixed epoxy-impregnated thin section of Core C-2 from West Side, Ground Level showing: (a) fine, hair-like, discontinuous shrinkage microcracks in the dense Portland cement paste of grout, some are marked with arrows in all rows; (b) the intimate interface between grout and concrete (bottom row), (d) microcracking in grout near the grout-concrete interface (bottom row), and (d) carbonated surface region of concrete at the top, right beneath the grout-concrete interface (bottom row).

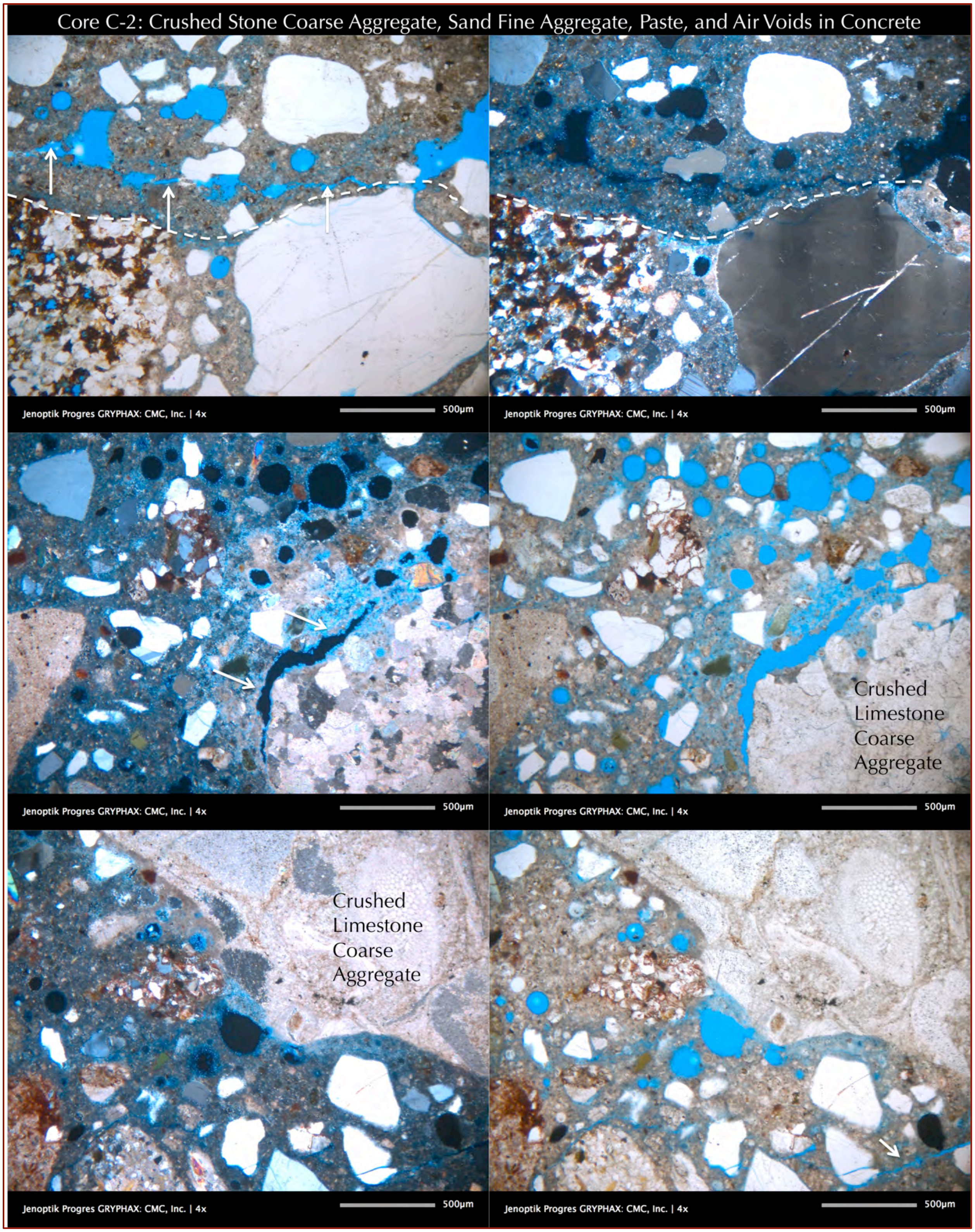

Figure 17: Photomicrographs of blue dye-mixed epoxy-impregnated thin section of Core C-2 from West Side, Ground Level showing: (a) fine, hair-like, discontinuous shrinkage microcracks in the dense Portland cement paste of grout, some are marked with arrows in the top row, immediately above the grout-concrete interface (top row); (b) crushed limestone coarse aggregate, natural siliceous-calcareous sand fine aggregate, Portland cement paste, and air voids in concrete beneath the grout (middle and bottom rows).

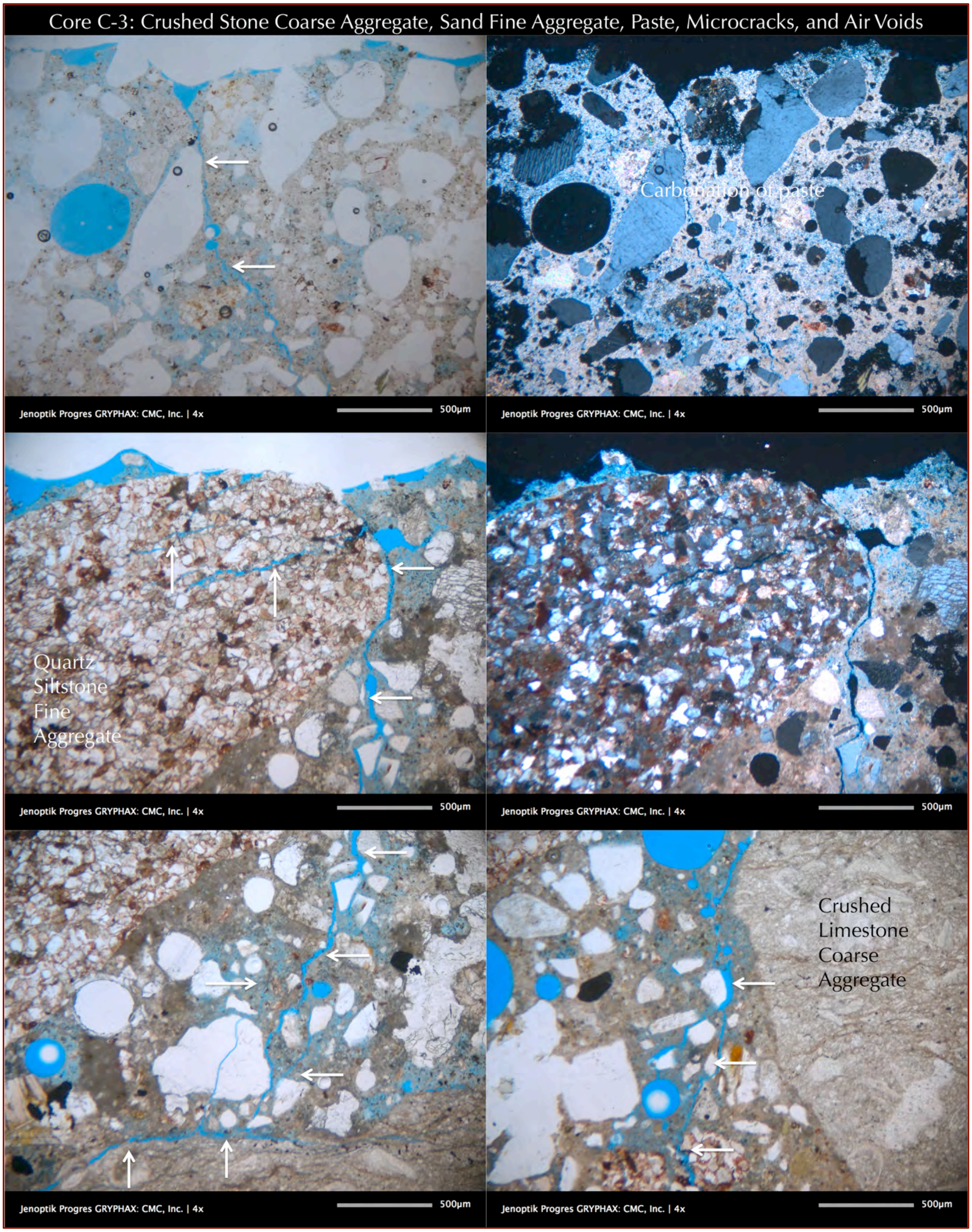

Figure 18: Photomicrographs of blue dye-mixed epoxy-impregnated thin section of Core C-3 from North Side, 2nd Level showing: (a) carbonated surface region of concrete with a few vertical fine, discontinuous, shallow-depth shrinkage microcracks (some marked with arrows in all three rows); and (b) crushed limestone coarse aggregate, natural siliceous-calcareous sand fine aggregate, Portland cement paste, and air voids (highlighted by blue dye-mixed epoxy) in middle and bottom rows.

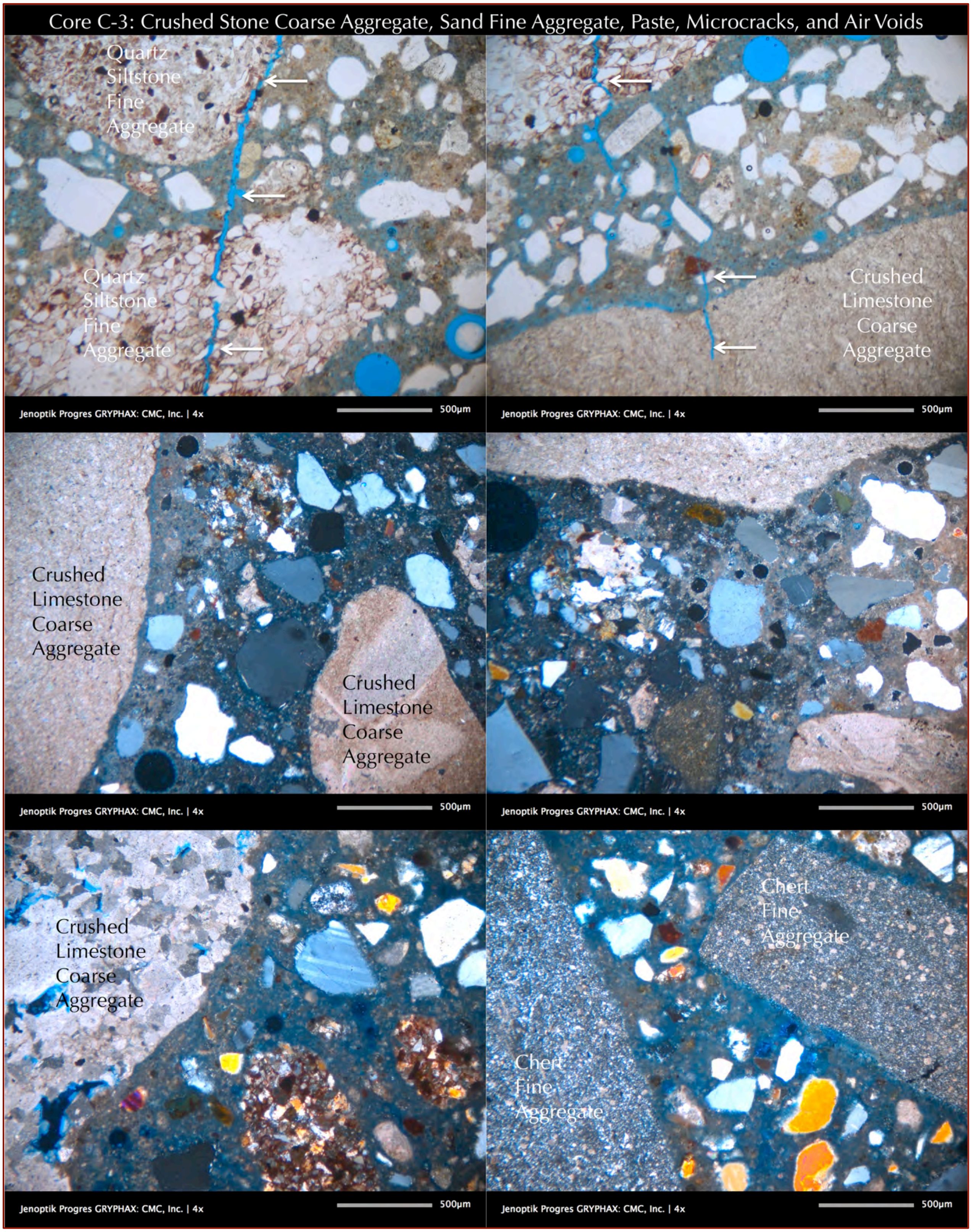

Figure 19: Photomicrographs of blue dye-mixed epoxy-impregnated thin section of Core C-3 from North Side, 2nd Level showing crushed limestone coarse aggregate, quartz, quartz siltstone, ferruginous quartz siltstone, and chert particles in fine aggregate, and non-carbonated interior Portland cement paste, often with some fine, discontinuous, shrinkage microcracks (some are highlighted by the blue dye-mixed epoxy and marked with arrows in top row).

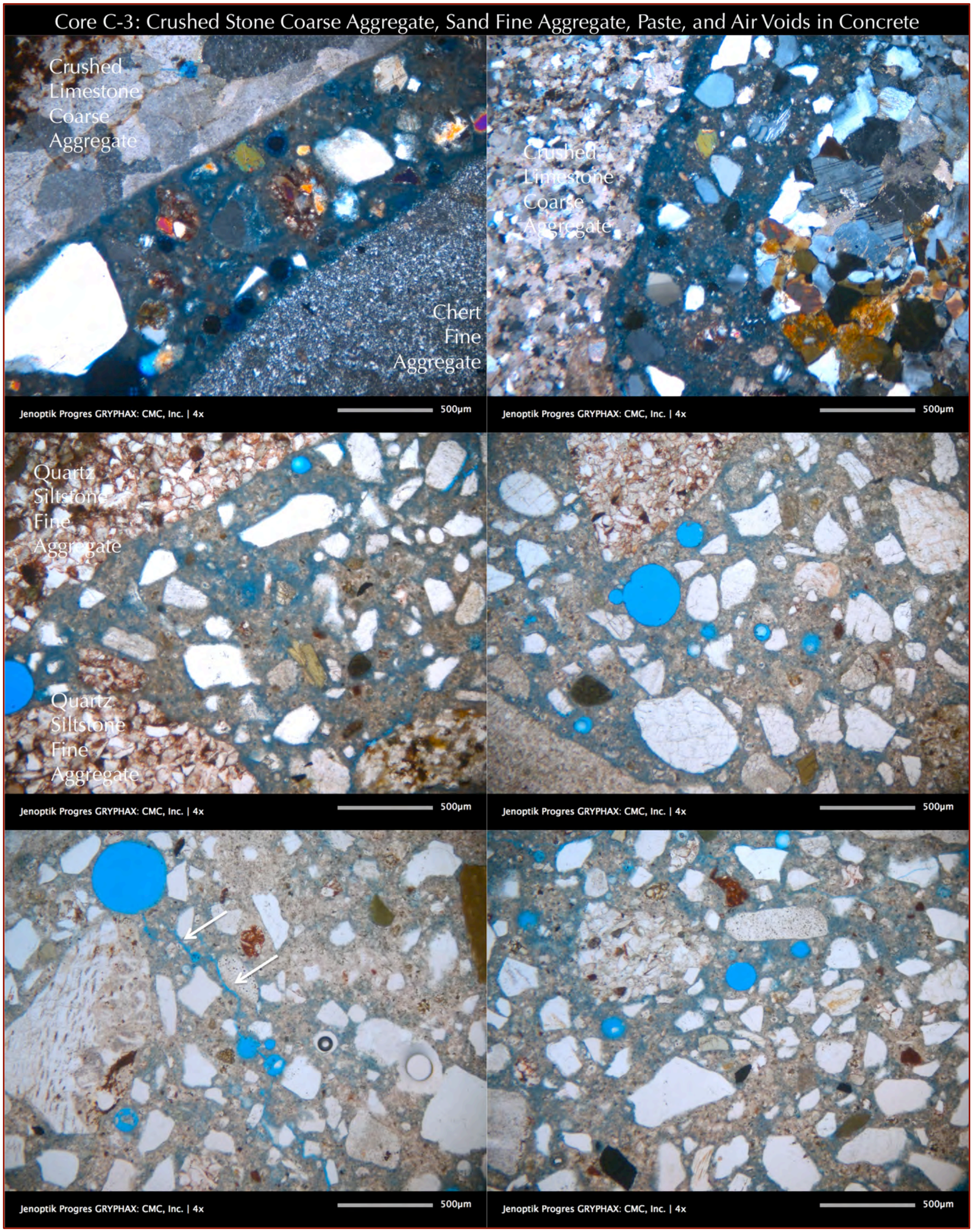

Figure 20: Photomicrographs of blue dye-mixed epoxy-impregnated thin section of Core C-3 from North Side, 2nd Level showing crushed limestone coarse aggregate, quartz, granite, and quartz siltstone particles in fine aggregate, and non-carbonated interior Portland cement paste, often with some fine, discontinuous, shrinkage microcracks highlighted by the blue dye-mixed epoxy (some are marked with arrows in the bottom row).

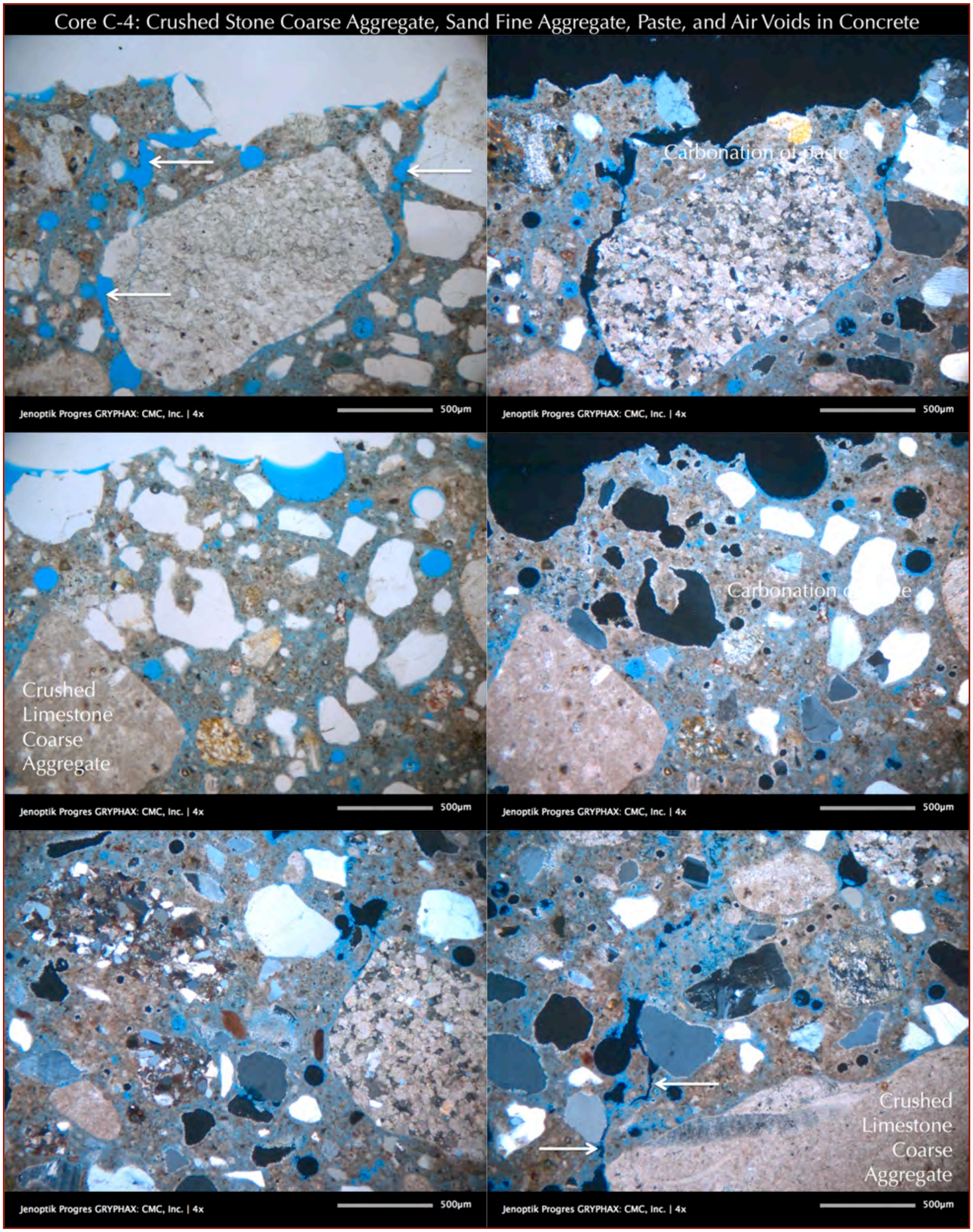

Figure 21: Photomicrographs of blue dye-mixed epoxy-impregnated thin section of Core C-4 from East Side, 2nd Level showing: (a) carbonated surface region of Portland cement paste, often with a few vertical fine, discontinuous, hair-like shrinkage microcracks that are highlighted by the blue dye-mixed epoxy and some are marked with arrows in top and bottom rows; (b) crushed limestone coarse aggregate and natural siliceous-calcareous sand fine aggregate particles, Portland cement paste, and air voids (highlighted by the blue dye-mixed epoxy).

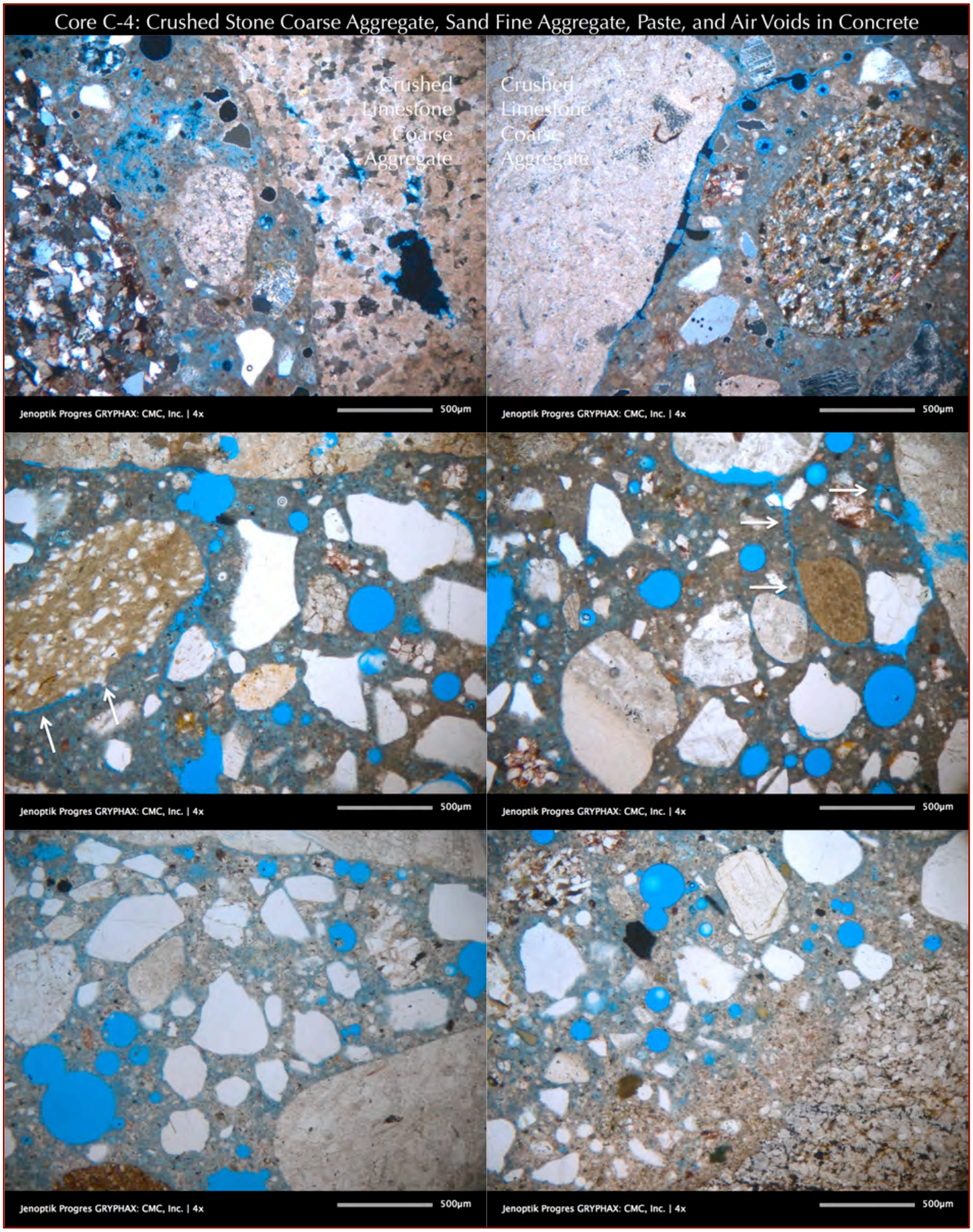

Figure 22: Photomicrographs of blue dye-mixed epoxy-impregnated thin section of Core C-4 from East Side, 2nd Level showing crushed limestone coarse aggregate, natural siliceous-calcareous sand fine aggregate, carbonated (top row) and non-carbonated (middle and bottom rows) Portland cement paste, and air voids (highlighted by the blue dye-mixed epoxy) and some fine, discontinuous, hair-like shrinkage microcracks in paste (some are marked with arrows in middle row).

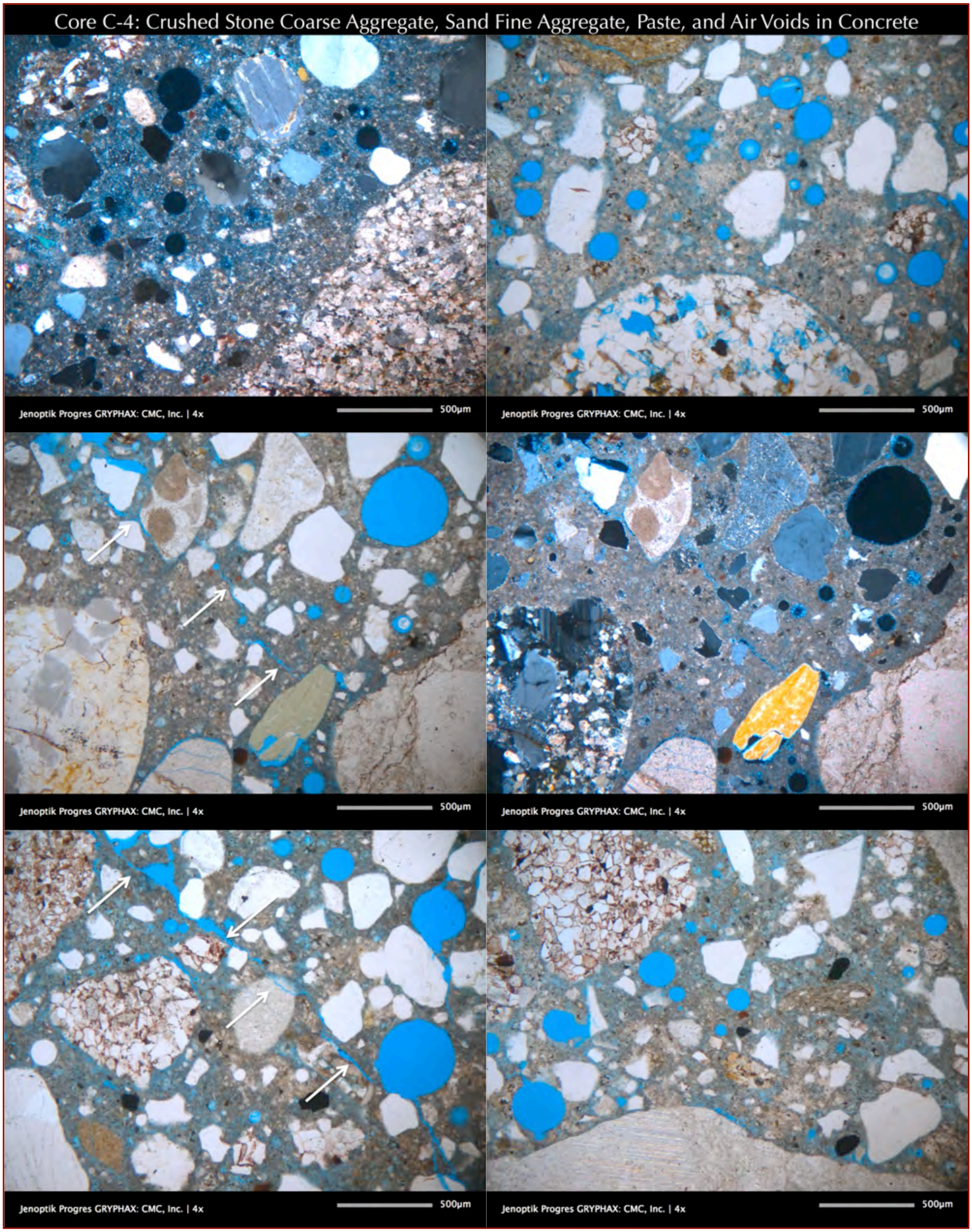

Figure 23: Photomicrographs of blue dye-mixed epoxy-impregnated thin section of Core C-4 from East Side, 2nd Level showing crushed limestone coarse aggregate, natural siliceous-calcareous sand fine aggregate, Portland cement paste, and air voids (highlighted by the blue dye-mixed epoxy) and some fine, discontinuous, hair-like shrinkage microcracks in paste (some are marked with arrows in middle row).

AIR-VOID ANALYSES

Air-void analyses of concrete cores *a la* ASTM C 457 determined the concretes in all cores to be air-entrained. The following table provides the determined air-void parameters of concretes in the cores:

Air Void System and Parameters	C-1 South Side, Ground Level	C-2 (Concrete) West Side, Ground Level	C-3 North Side, 2nd Level	C-4 East Side, 2nd Level
Air Entrainment	Air-Entrained	Air-Entrained	Air-Entrained	Air-Entrained
Air-Void System	Excellent	Good	Good	Excellent
Total Air Content, %, Determined	7.07	5.39	5.66	7.14
Entrained Air Content, %, Determined	6.36	4.39	4.22	6.20
Paste Content, %, Determined	35.41	37.49	25.44	32.64
Paste-Air Ratio	5.009	11.057	9.571	7.769
Specific Surface, in.^{2}/in.^{3}	949	1149	834	1772
Air-Void Spacing Factor, in.	0.0049	0.0058	0.0075	0.0032

Table 4: Properties and parameters of air void system of concretes in the cores. Entrained air voids are defined as discrete spherical or near-spherical voids of sizes 1 mm or less. Common industry (e.g., ACI, ASTM) requirements for a concrete containing $^3/_4$ in. nominal maximum size coarse aggregate and exposed to a moist outdoor environment of cyclic freezing and thawing are an air content of 6±1$^1/_2$ percent, a minimum specific surface of 600 in.^{2}/in.^{3} and a maximum void-spacing factor of 0.008 in.

Air occurs as: (i) numerous fine discrete, spherical and near-spherical voids having sizes of up to 1 mm, and (ii) coarse, near-spherical and irregularly shaped voids of sizes coarser than 1 mm. The former voids are characteristic of entrained air and the latter ones are entrapped air. Air-void systems of concretes are suggestive of intentional addition of an air-entrained agent in the mix.

Overall air-void systems of concretes are better in Cores C-1 and C-4 than in Cores C-2 (concrete) and C-3. The former two cores have much finer air bubbles, more amount and uniform distribution of air, whereas the latter two cores have relatively lesser air and coarser air void system. All four cores, however, show air void systems that should provide necessary durability of concrete in an environment of cyclic freezing and thawing at critically saturated conditions.

Therefore, concretes in cores C-1 from south side ground level and C-4 from east side 2nd level have overall higher air contents and finer air-void systems than the concretes from C-2 and C-3. Specific surfaces are all higher than the minimum recommended value of 600 in.^{2}/in.^{3}, and the air void-spacing factors are all less than the maximum recommended value of 0.0080 in.

Figures 24 through 28 show air contents, air-void systems, and distribution of air bubbles throughout the depths of four cores (including the grout portion in Core C-2).

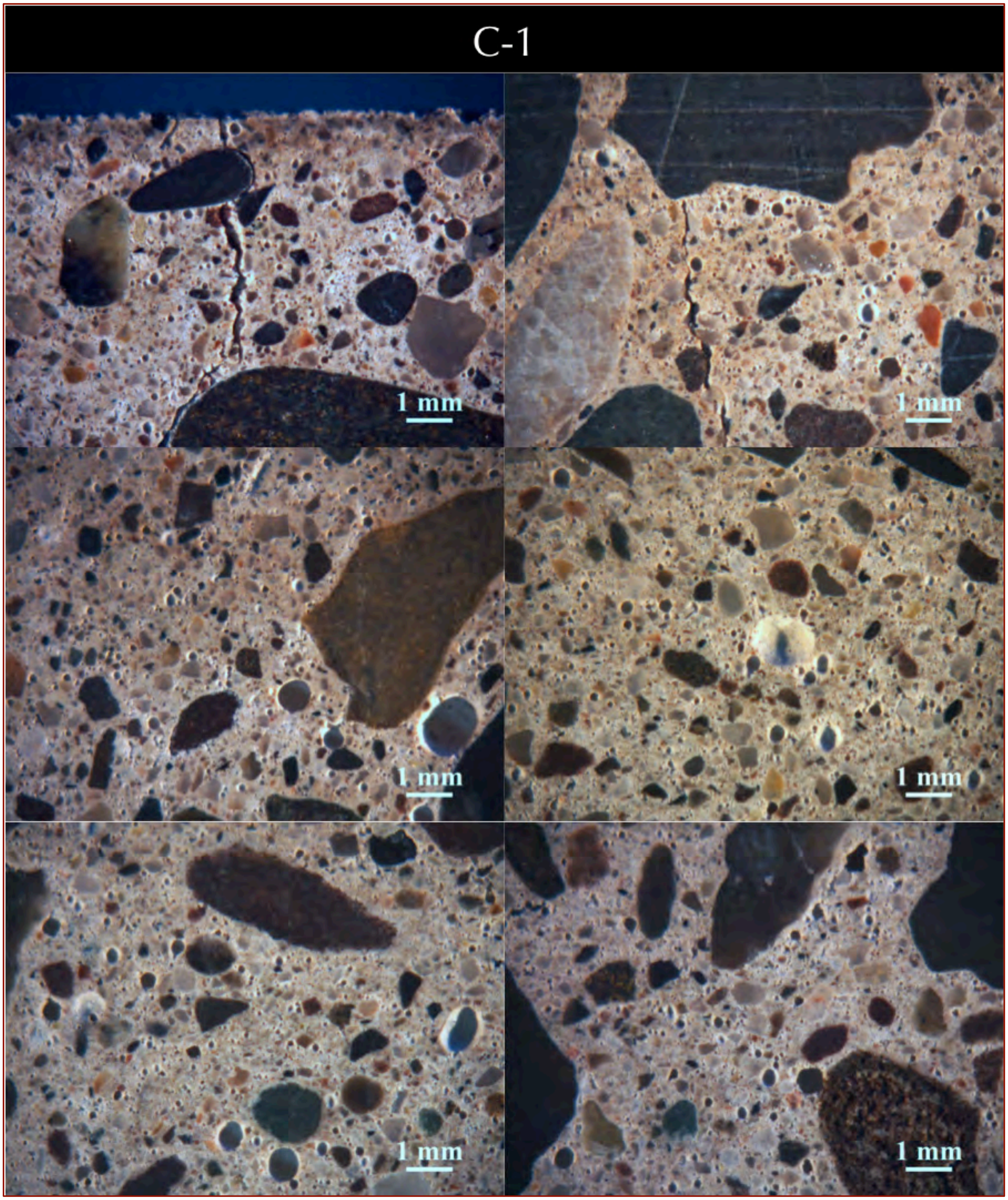

Figure 24: Photomicrographs of lapped cross section of Core C-1 South Side, Ground Level showing the air-entrained nature of concrete and distribution of numerous, fine, discrete, spherical and near-spherical entrained air voids and a few coarse near-spherical and irregularly-shaped entrapped air voids. This core has a fine air-void system.

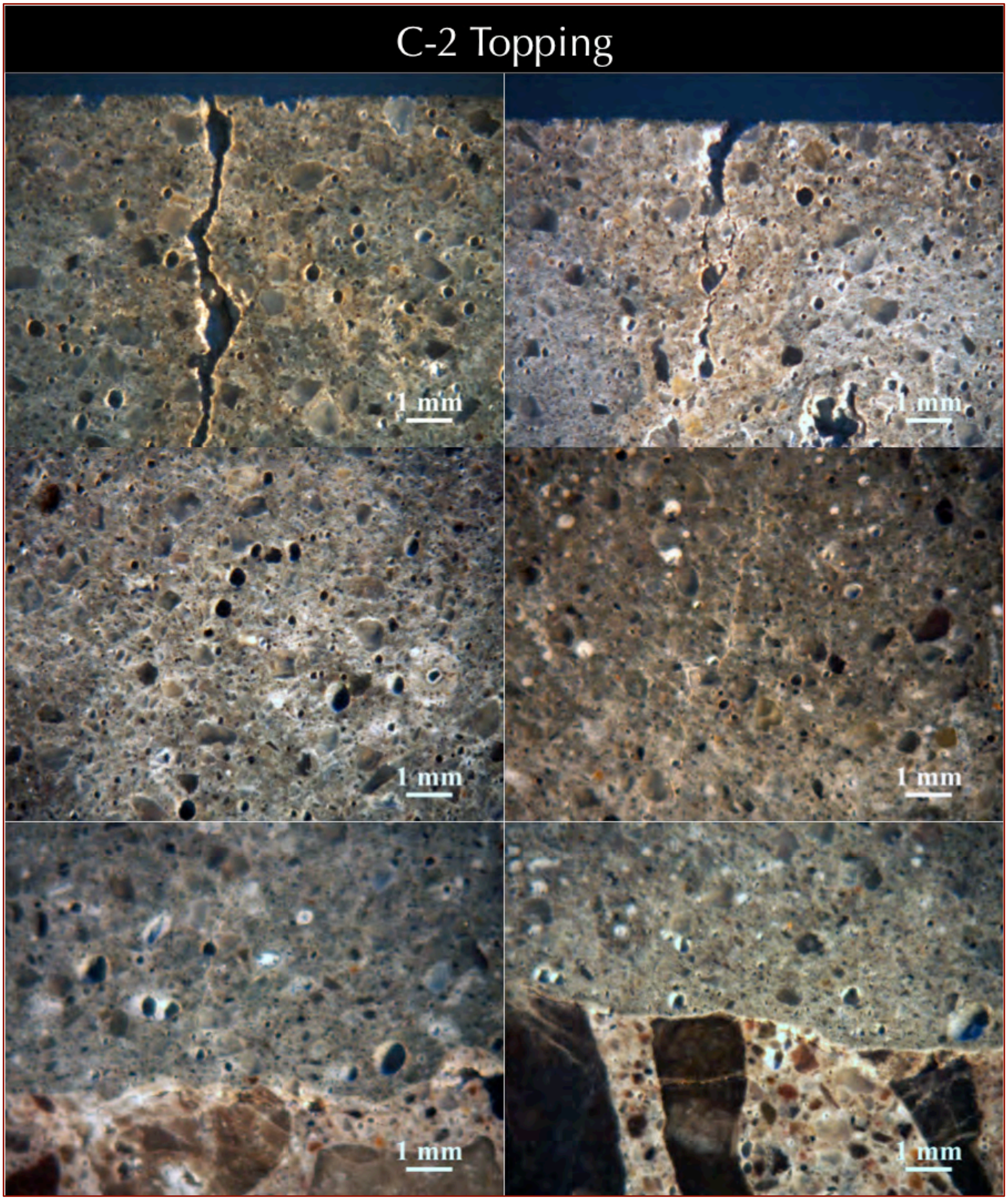

Figure 25: Photomicrographs of lapped cross section of Core C-2 Topping Grout from West Side, Ground Level showing the air-entrained nature of the top grout portion of the core and distribution of numerous, fine, discrete, spherical and near-spherical entrained air voids and a few coarse near-spherical and irregularly-shaped entrapped air voids. Also notice a vertical shrinkage crack at the top few millimeters of grout in the top row, and, grout-concrete interface in the bottom row.

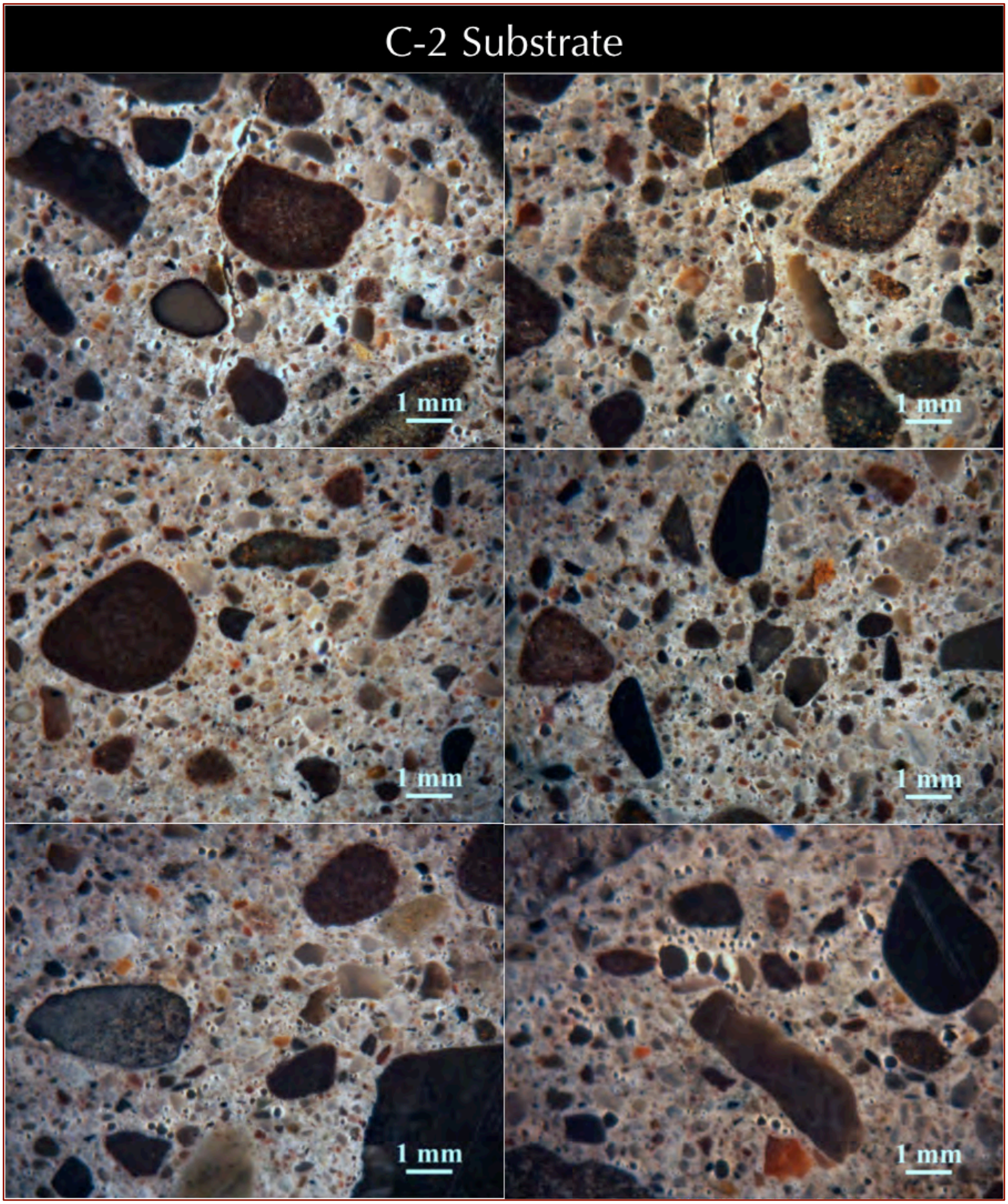

Figure 26: Photomicrographs of lapped cross section of Core C-2 Substrate from West Side, Ground Level showing the air-entrained nature of concrete and distribution of fine, discrete, spherical and near-spherical entrained air voids and a few coarse near-spherical and irregularly-shaped entrapped air voids. Notice some fine shrinkage microcracks in concrete substrate in the top row.

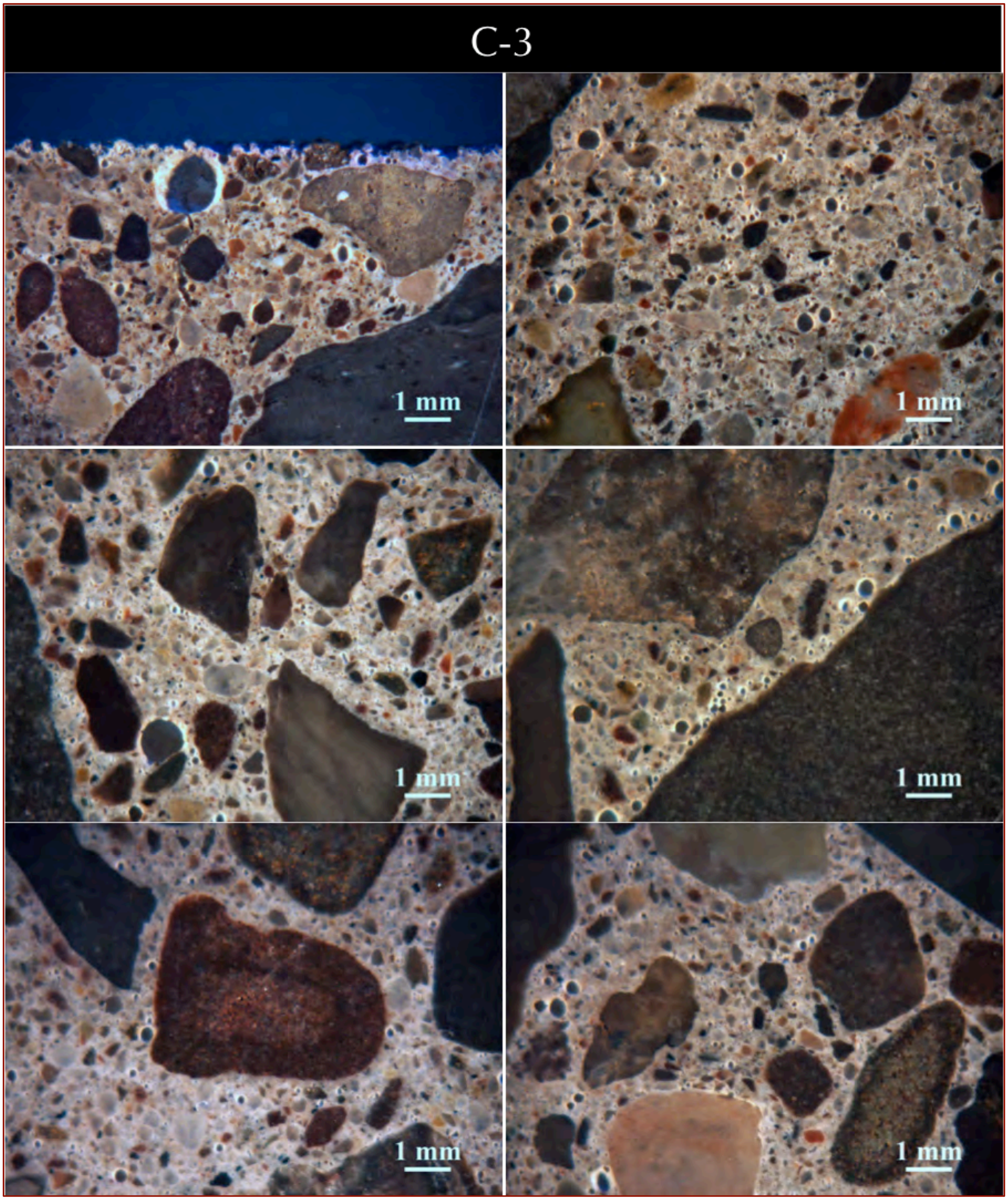

Figure 27: Photomicrographs of lapped cross section of Core C-3 North Side 2nd Level showing the air-entrained nature of concrete and distribution of fine, discrete, spherical and near-spherical entrained air voids and a few coarse near-spherical and irregularly-shaped entrapped air voids.

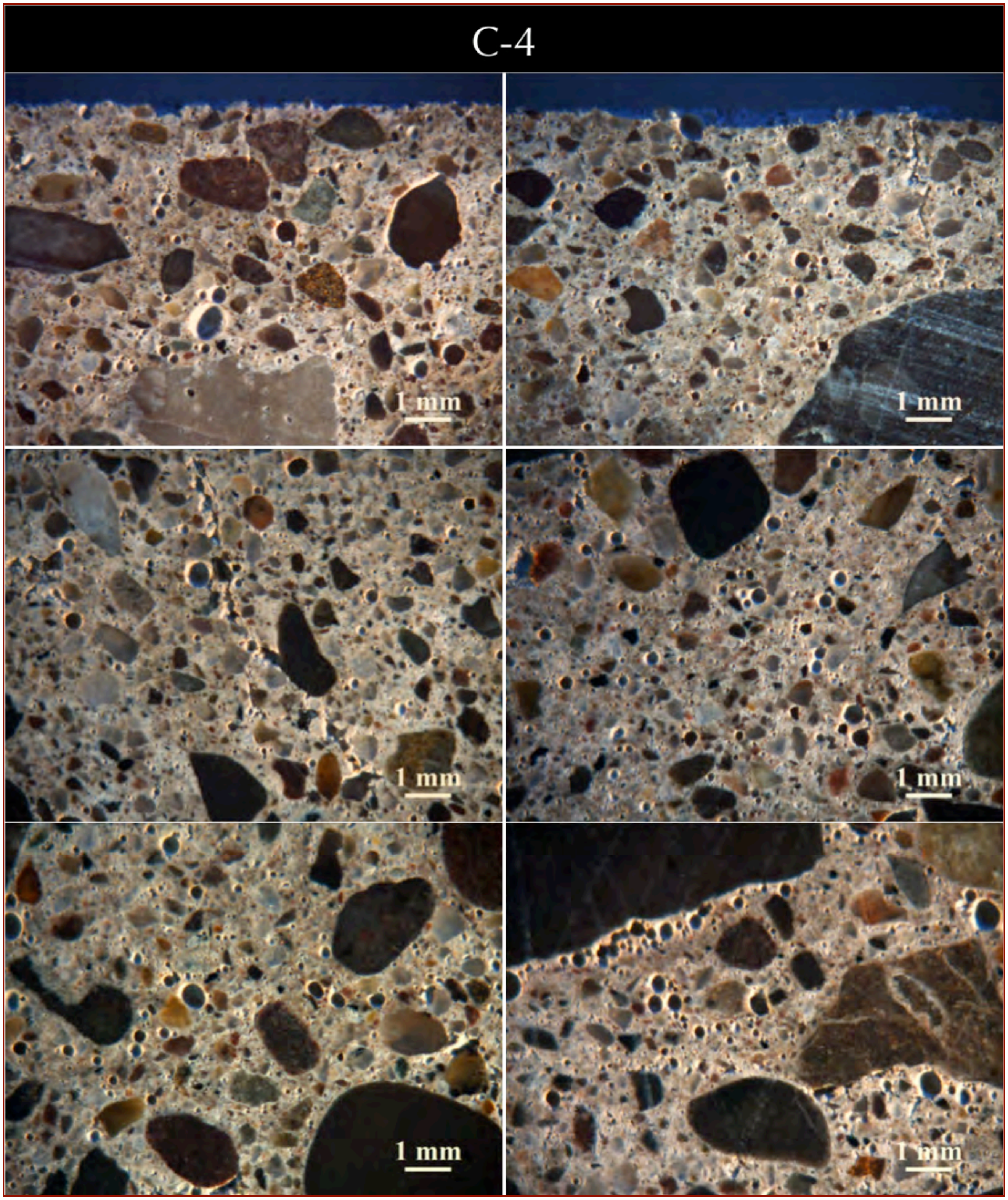

Figure 28: Photomicrographs of lapped cross section of Core C-4 East Side 2nd Level showing the air-entrained nature of concrete and distribution of numerous, fine, discrete, spherical and near-spherical entrained air voids and a few coarse near-spherical and irregularly-shaped entrapped air voids. This core has the maximum air voids and a fine air-void system.

CONCLUSIONS

Concretes in all four cores are air-entrained and made using crushed limestone coarse aggregates having nominal maximum sizes of 3/4 in. (19 mm); natural siliceous-calcareous sand fine aggregates having nominal maximum sizes of 3/16 in. (4.8 mm); Portland cement pastes having estimated cement contents of 6 to 6 1/2 bags per cubic yard, and water-cement ratios of pastes of 0.50 to 0.55; and determined air contents of 5.4 to 7.1 percent.

Concretes in all cores are air-entrained having air-void systems consisting of numerous fine, discrete, spherical and near spherical entrained air voids, and a few coarse and irregularly shaped entrapped air voids. Concretes in cores C-1 from south side ground level and C-4 from east side 2nd level have overall higher air contents and finer air-void systems than the concretes from C-2 and C-3. Specific surfaces are all higher than the minimum recommended value of 600 in.^{2}/in.^{3}, and the air void-spacing factors are all less than the maximum recommended value of 0.0080 in.

Carbonation of concrete is judged to be higher than that normally found in a well-consolidated, well-cured concrete made using a reasonable water-cementitious materials ratio of 0.45 or less. Depths of carbonation measured on thin sections of cores are found to be: (i) as deep as 35 mm in C-1, (ii) merely 2 mm in the dense top grout in C-2, except along the visible vertical shrinkage-related crack on the grout where carbonation of paste along the crack walls has extended to a depth of 15 mm, (iii) 2 mm deep carbonation from the scarified concrete surface beneath the grout topping in C-2, (iv) 15 mm deep from the top surface of concrete in C-3, and (v) 22 mm deep in Core C-4. These depths are indicative of a concrete that has lesser resistance to penetration of atmospheric carbon dioxide and hence more permeability to CO_2 than desired for prevention of any carbonation-induced corrosion of reinforcing steel in concrete. Although there is no evidence of any corrosion of steel in Core C-4, which has a No. 4 reinforcing steel at a depth of 3 in. based on these deep carbonation depths, the possibility of such corrosion if steel reinforcement is present within the top 1 to 2 in. is present.

Along with this evidence of deep carbonation, another microstructural evidence found in all four cores also indicate an inherent water-cement ratio of concrete that has not only increased permeability of concrete to CO_2 but also helped to form this microstructure. This evidence is the detection of fine, hair-like discontinuous microcracks that are detected in the paste fractions of all cores and are judged to be present at frequencies higher than that anticipated in a concrete made using a reasonable maximum water-cement ratio of 0.45. Deep carbonation and higher frequency of microcracking are thus both indicative of an inherent high water-cement ratio of concrete, which is consistent with the estimated values of 0.50 to 0.55. Composition, density, hardness, texture, lustre, and porosity of pastes, and appearance and behavior of cores during sectioning and lapping also corroborated the above conclusions.

REFERENCES

ASTM C 856 "Standard Practice for Petrographic Examination of Hardened Concrete," Vol. 4.02, ASTM International, West Conshohocken, PA, 2014.

Jana, D., and Cole, A.A., "Microscopy: A Practical Solution to Concrete Problems," *Bulletin of Concrete Industry Board*, September 1997, pp. 18-22.

Jana, D., "Petrography: A Powerful Tool For Solving Common Concrete Problems," *Civil Engineering NEWS*, March 1997, pp. 40-44.

Jana, D., "Sample Preparation Techniques in Petrographic Examinations of Construction Materials: A State-of-the-art Review," *Proceedings of the 28th Conference on Cement Microscopy*, International Cement Microcopy Association, Denver, Colorado, pp. 23-70, 2006.

Jana, D., "Concrete, Construction, or Salt – Which Causes Scaling? Part 2: Importance of Finishing Practices," *Concrete International*, December 2004, pp. 51-56, American Concrete Institute.

Jana, D., "Petrography and Concrete Repair – A Link is Needed," Point of View Publication in *Concrete International*, American Concrete Institute, pp. 37-39, January 2005.

Jana, D., and Erlin, B, "Delamination – The Sometime Curse of Entrained Air," *Concrete Construction*, January 2005, pp. 101-106.

✪ ✪ ✪ END OF TEXT ✪ ✪ ✪

END OF REPORT[1]

[1] The CMC logo is made using a lapped polished section of a 1930's concrete from an underground tunnel in the U.S. Capitol.